



A study of brain networks for autism spectrum disorder classification using resting-state functional connectivity

Xin Yang ^{a,*}, Ning Zhang ^b, Paul Schrader ^c

^a Middle Tennessee State University, Murfreesboro, TN, USA

^b St. Ambrose University, Davenport, IA, USA

^c Southern Arkansas University, Magnolia, AR, USA



ARTICLE INFO

Keywords:

Functional connectivity

Brain networks

rs-fMRI

ASD

ROIs ABIDE

Deep Neural Network

ABSTRACT

This paper presents a comprehensive and practical review of autism spectrum disorder (ASD) classification using several traditional machine learning and deep learning methods on data from the Autism Brain Imaging Data Exchange (ABIDE) repository. The objective of this study was to investigate different brain networks and determine their functional connectivity to distinguish between subjects with ASD and those considered typically developing (TD). In the experiments of this paper, functional connectivity was used as a classification feature for 871 resting-state functional magnetic resonance imaging (rs-fMRI) samples collected from the ABIDE repository. The methodology and results of this paper have three main parts.

First, we reviewed eight different brain parcellation techniques used for ASD classification from structural, functional, and data-driven perspectives to identify the most promising brain atlas. Second, we evaluate the stability and efficiency of the correlation, partial correlation, and tangent space functional connectivity metrics, and identify the most stable functional connectivity metric. Third, we compared four different supervised learning models used in the ASD classification domain and evaluated the learning performance of each model. In summary, our experimental results show that Bootstrap Analysis of Stable Clusters (BASC) provides the most predictive power for ASD classification, while the correlation metric is the most stable candidate among those models considered. Furthermore, by comparing different classifiers, we conclude that among all the experimentally compared classifiers in this paper, the kernel support vector machine (kSVM) is the optimal classifier for classifying ABIDE fMRI data. The highest sensitivity 64.57% is identified in Table 7. This result was produced using the correlation metric with functional atlas BASC444 and RBF kernel SVM. The corresponding specificity is 73.61%, and the accuracy is 69.43%. Overall, this is the optimal result.

Contents

1. Introduction	2
2. Brain network	4
2.1. Predefined atlases.....	4
2.2. Data-driven method.....	5
3. Resting-state functional connectivity.....	5
4. Machine learning methods.....	6
4.1. Supervised learning classifiers	6
4.2. Logistic regression	6
4.3. Support Vector Machine.....	7
4.4. Deep neural network	7
5. Experiments	7
5.1. The ABIDE dataset	7
5.2. Data preprocessing	8
5.3. Experimental design pipeline.....	8
5.4. Five-Fold-Cross-Validation (FFCV).....	8
5.5. Receiver Operating Characteristic (ROC) Curve.....	9

* Corresponding author.

E-mail addresses: Xin.Yang@mtsu.edu (X. Yang), zhangning@sau.edu (N. Zhang), paulschrader@saumag.edu (P. Schrader).

5.6. Experimental results	10
6. Conclusion	13
CRediT authorship contribution statement	14
Declaration of competing interest.....	14
Appendix A. Supplementary data	14
References.....	16

1. Introduction

Our brain is a complex network consisting of numerous spatially distributed but functionally related brain regions. While supervising and performing different tasks, brain regions effectively coordinate with each other at regular intervals, forming a complex network of brain connections (Riaz, Asad, Alonso, & Slabaugh, 2020). Many psychiatric disorders are due to damage or lesions in the nerves of the brain. Therefore, a complex understanding of brain networks is crucial to decode the relationship between mental functioning and brain processes in psychiatric disorders. In recent decades, research on the brain has become a pressing public health issue. Scientists and research institutions have invested tremendous experience and resources to conduct research in order to better understand the working mechanisms of the brain. As research intensified, neuroimaging was gradually developed. With the rise of neuroimaging, many research techniques in neuroimaging have emerged. One of these very popular methods is functional magnetic resonance imaging (fMRI).

fMRI is a technique that uses magnetic resonance imaging to measure brain activity by computing changes in the local oxygenation of blood which corresponds to the amount of neighboring brain activity. Since its development in the early 1990s, fMRI has become the most popular imaging brain function method (Poldrack, Mumford, & Nichols, 2011). The reason for its overwhelming popularity is that fMRI provides an entirely safe and non-invasive method to image brain activity with reasonable spatial and temporal resolution compared to the ionizing radiation methods (e.g., computed tomography (CT) or positron emission tomography (PET)). With the establishment of fMRI, a revolution occurred in the ability to see inside the human brain. Cognitive neuroscientists around the world quickly adopted fMRI as the primary imaging tool for neurocognition studies.

The initial development of the fMRI technique was driven by research interested in the brain's response to external events or mental stimuli. As a result, most initial investigations focused on the measurement of responses evoked by external events. It was not until half a decade after its invention that neuroscientists began to explore the metrics of functional connectivity between brain regions of fMRI time series recorded during rest-state. Analyzing brain connectivity with functional magnetic resonance imaging (fMRI) data provides a means to understand how spatially distributed brain regions interact and work together to create mental function.

Biswal and his colleagues (Biswal, Kylen, & Hyde, 1997; Biswal, Yetkin, Haughton, & Hyde, 1995) were the first to demonstrate that the left and right hemispheric regions of the primary motor cortex are not silent during rest. In their studies, they showed that the functionally related brain regions exhibit a correlation of low-frequency fluctuations in the resting state. They hypothesized that the functional connectivity demonstrated in the motor cortex is a general phenomenon and not due to external motor tasks. This suggested that correlations in resting-state activity can provide meaningful insight into the neural function even without external events or mental stimuli.

Since 2000, there has been an explosion in the use of resting-state fMRI data to study brain function. In Damoiseaux et al. (2006), Damoiseaux and his colleagues found ten rest patterns with relatively large coherent fluctuations in the rs-fMRI data of healthy subjects. These rest patterns consisted of regions known to be involved in motor function, visual processing, executive functioning, auditory processing, and the

default-mode network. Their findings align with other research, which has consistently shown coherent fluctuations in the blood oxygen level-dependent (BOLD) signal within the specific neuroanatomical systems (Biswal et al., 1997, 1995; Damoiseaux et al., 2006).

These early findings drove the subsequent studies to move away from a sole focus on event-design tasks. Scientists have gradually recognized that it is useful to investigate whether the patterns identified in resting-state fMRI data present the same characteristics under different conditions. For example, in Greicius, Srivastava, Reiss, and Menon (2004), they have found that the hippocampus appears to play a prominent role in the default-mode network, and the corresponding network activity is deficient in Alzheimer disease (AD) subjects compared to healthy elderly controls. These results indicate that the hippocampus could be a potential clinical marker of AD. Since no complicated experimental design is required, the use of resting-state fMRI to investigate the influence of disease on the brain has obvious clinical advantages. Further studies have shown that rs-fMRI has become an essential technique to analyze the brain's spontaneous activity and intrinsic functional connectivity (Al-Zubaidi, Mertins, Heldmann, Jauch-Chara, & Münte, 2019).

Autism spectrum disorder (ASD) is a neurological and developmental disorder that is characterized by the impaired development of social interactions and communication skills. According to estimates from the Center of Disease Control's (CDC) Autism and Developmental Disabilities Monitoring Networks (ADDM), about 1 in 54 children has been identified with ASD in the United States. With an increasing number of families around the world being affected by this disease, the need for studies of ASD is imperative. ASD can be detected as early as 18 months or younger. However, many children are not fully diagnosed until an older age for a variety of socioeconomic reasons. This delay means that the children with ASD might not get the early intervention they need. According to a current CDC report, early intervention could provide a suitable treatment plan and aid in the later rehabilitation of ASD patients (Boat & Wu, 2015).

Although genetic and environmental factors are suspected, and many causes of ASD have been proposed, the exact etiology of ASD is still unclear. Furthermore, the diagnosis of ASD is challenging and complicated. Its diagnosis is generally made based on comprehensive behavioral assessments by a specialist in child psychiatry or psychology. There are several sets of practical guidelines that govern the screening and diagnosis of ASD. These practice guidelines suggest that the comprehensive behavioral evaluations should involve observations of the child's behavior, testing of cognition, speech and language, hearing, vision, motor function, medical and family histories, etc. (McClure et al. 2014). In recent years, the role of genetic factors in ASD etiology has been increasingly recognized, although the genetics of ASD appears to be very complex. Nonetheless, behavioral evaluations may also involve genetic testing.

These conventional approaches have elucidated many aspects of ASD. However, recent advances in neuroimaging data raise the possibility of deciphering additional and complementary information from fMRI data. In addition to the behavioral assessments, investigation of functional connectivity using fMRI data may help further understand ASD cognitive and behavioral profiles possibly characterizing the neural basis impaired by ASD.

In 2004, Just and his colleagues conducted seminal experiments to compare brain activation during sentence comprehension between ASD and control subjects using fMRI data (Just, Cherkassky, Keller,

& Minshew, 2004). Their studies showed that the ASD participants have less activation in the left inferior frontal gyrus (LIFG) and more activation in the left posterior superior temporal gyrus (LPSTG) than the control group. Additionally, the functional connectivity was lower throughout the cortical language system among the ASD patients than in the control. These results suggested that the overall coordination and communication between cortical areas are lower in the ASD group. They proposed that ASD is a cognitive and neurobiological disorder marked and caused by under-functioning integrative circuitry resulting in a deficit of information integration at the neural and cognitive levels.

These fMRI findings in ASD have shifted focus away from behavioral assessment toward neuroimaging studies. Since then, there has been an explosion in the use of fMRI data to characterize ASD etiology. An increasing number of studies have shown that social and communicative impairments are associated with cortical networks' functioning and connectivity. The cortical underconnectivity theory has been proposed as an explanatory model for ASD which suggests that abnormal functional connectivity among brain regions may be responsible for ASD patients' performance in cognitive and social tasks (Courchesne et al., 2007; Kleinhans et al., 2008; Weng et al., 2010).

Traditionally, fMRI analysis methods have focused on characterizing the relationship between cognitive variables and individual brain voxels. However, there are limits on what can be learned about cognitive states by examining voxels in isolation. In 2006, Norman and his colleagues proposed a new powerful approach known as multi-voxel pattern analysis (MVPA), which attempts to analyze the information present in patterns of activity rather than the response at individual voxels (Norman, Polyn, Detre, & Haxby, 2006). Nowadays, MVPA has become a leading technique in the analysis of neuroimaging data. It has been extensively used to investigate how a pattern of brain activity is related to different cognitive states (Cox & Savoy, 2003; Duda, Hart, & D.G., 2012; Kana, Libero, & Moore, 2011).

The typical MVPA applications in fMRI involve using pattern recognition and machine learning algorithms to expose functional relationships between brain response patterns and the perceptual, cognitive, or behavioral states of a subject. The relationships are expressed in terms of a label which may assume classification or regression values. The learned functional relationship is then used to predict the unseen labels from a new dataset (Formisano, De Martino, & Valente, 2008).

Deep learning was developed from artificial neural networks, whose origins date back to the 1940s (Du, Cai, Wang, & Zhang, 2016). In 2006, Hinton et al. proposed the concept of deep learning (Hinton & Salakhutdinov, 2006). They demonstrated that deep learning would be significantly more efficient, if computers were "fast enough", and datasets were "big enough". Since then, deep learning algorithms have dramatically improved the state-of-the-art traditional machine learning algorithms in many fields such as speech recognition (Amodei et al., 2016; Graves, Mohamed, & Hinton, 2013; Hannun et al., 2014), object recognition (Eitel, Springenberg, Spinello, Riedmiller, & Burgard, 2015; Liang & Hu, 2015; Socher, Huval, Bath, Manning, & Ng, 2012), drug discovery (Gawehn, Hiss, & Schneider, 2016; Zhang, Tan, Han, & Zhu, 2017), and genomics (Eraslan, Avsec, Gagneur, & Theis, 2019; Zou et al., 2019). Compared with traditional machine learning methods, deep learning has enhanced learning capabilities that utilize datasets more effectively for feature extraction (Du et al., 2016). Currently, deep learning algorithms have become heavily studied within the field of neuroscience involving fMRI. They have been successfully applied to both voxel-based classification (Jang, Plis, Calhoun, & Lee, 2017) and functional connectivity-based classification (Kim, Calhoun, Shim, & Lee, 2016; Meszlényi, Buza, & Vidnyánszky, 2017).

In Table 1, we summarize the recent research related to the classification of autism. Before the ABIDE data was released, there were few sample data people could study. For example, Wang et al. analyzed 29 ASD and 29 TC (Wang, Chen, & Fushing, 2012), Uddin et al. analyzed 20 ASD and 20 TC (Uddin et al., 2013), they both used the traditional classifier logistic regression. With the access to ABIDE database, more

and more articles began to quote ABIDE's public data. Zhou, Yu, and Duong (2014) and Chen et al. (2015) both used the traditional classifier SVM, but they only reported accuracy. For the classification of autism, sensitivity and specificity are also very important metrics. In 2015, Dodero et al. proposed to use the grassman manifold method for classification, and they have obtained good results in terms of sensitivity, but at the expense of specificity (Dodero, Sambataro, Murino, & Sona, 2015). In addition, their data sample only has 43 ASD and 37 TC. In 2017, Guo et al. used the DNN classifier, an accuracy rate of 86.36% was obtained, but their sample only had 55 ASD and 55 TC, and they did not report sensitivity and specificity. With the increase of ABIDE's public data, starting from 2017, many articles began to use all ABIDE's 1112 samples or 871 samples after the quality screening. Dvoneck et al. used the LSTM model to obtain an accuracy of 68.5% but did not give sensitivity and specificity results (Dvornek, Ventola, Pelphrey, & Duncan, 2017). In 2018, Heinsfeld et al. applied DNN to obtain 70% accuracy, 74% sensitivity, and 63% specificity (Heinsfeld, Franco, Craddock, Buchweitz, & Meneguzzi, 2018). However, we found that the result they reported was only a 10-fold cross-validation result and they did not repeat the experiment. Therefore, the stability of their DNN is questionable. To explore the potential of graph convolutional network, Yao et al. proposed a multi-scale triplet graph convolutional network (MTGCN) for brain functional connectivity analysis, and they obtained 67.30% accuracy, 64.20% sensitivity, and 70.40% specificity (Yao et al., 2019). To reduce the noises in rsfMRI raw data and establish functional network correspondence across various individual brains, Zhao et al. proposed a two-stage deep learning framework for both temporal and spatial analysis of ASD analysis, however, they only got an accuracy of 65.3% (Zhao, Dai, Zhang, Ge, & Liu, 2019). In 2020, Hu et al. proposed fuzzy multi-kernel clustering methods that use multiple hidden layers of information from the stacked auto-encoder. Their experiments were performed on the entire 1035 data subjects and achieved an accuracy of 61% (Lu, Liu, Wei, & Tu, 2020). In 2021, Yin et al. used DNN to obtain an accuracy of 79.2%, but again, they did not report the results of sensitivity and specificity (Yin, Mostafa, & Wu, 2021). Yang et al. used CNN to obtain an accuracy of 77.74% and a sensitivity of 78.57%. Both accuracy and sensitivity rate has been improved. However, the sample data only has 79 ASD and 105 TC (Yang et al., 2021). To model inter-site heterogeneity, Wang et al. proposed a novel multi-site clustering and nested feature extraction method (MC-NFE) for ASD detection, and they obtained 68.42% accuracy, 70.05% sensitivity, and 63.34% specificity (Wang, Yao, Ma, & Liu, 2022). Consider the heterogeneity of multi-site data, Zhang et al. proposed a deep learning approach combined with the F-score feature selection method for ASD diagnosis, however its accuracy is only 65.30% (Zhang et al., 2017).

Through literature study, we found that researchers continue to use traditional classifiers, and at the same time, more and more people are beginning to try to apply deep learning models. Therefore, this article will use several traditional machine learning and deep learning methods to conduct a comprehensive and practical review of the autism classification using ABIDE dataset. In addition, we also found that in the case of a small number of samples, a higher accuracy/sensitivity/specification rate will be obtained. When the sample increases, the corresponding rates decrease. Even if the accuracy/sensitivity/specification rate is relatively high, it is the result without repeated verification (Heinsfeld et al., 2018), or only the accuracy rate is reported (Yin et al., 2021). In this study, we studied 871 samples after the quality screening. To obtain reliable and repeatable results. We repeated 5-fold cross-validation 10 times. All source codes will be made public, and all results will be reproducible.

The purpose of the study in this paper is to use traditional machine learning methods and deep neural networks to analyze different brain networks to determine their functional connectivity in order to distinguish between ASD patients and typically developing (TD) participants. In our experiments, we used functional connectivity as

Table 1
Review summary.

Study	Participants	Data	Features	Correlation	Classifier	Accuracy	Sensitivity	Specificity
Wang et al. (2012)	29 ASD 29 TC	task fMRI	AAL	Unknown	LR	Unknown	82.8%	82.8%
Uddin et al. (2013)	20 ASD 20 TC	rsfMRI	group ICA	Unknown	LR	78%	75%	80%
Zhou et al. (2014)	127 ASD 153 TC (ABIDE)	rsfMRI	Integrated	Unknown	SVM	70%	Unknown	Unknown
Chen et al. (2015)	126 ASD 126 TC (ABIDE)	rsfMRI	Power	Pearson	SVM	<70%	Unknown	Unknown
Dodero et al. (2015)	42 ASD 37 TC (ABIDE)	rsfMRI	Power	Graph Laplacian	Grassmann Manifold	63.29%	73.81%	51.35%
Kassraian-Fard, Matthijs, Balsters, Maathuis, and Wenderoth (2016)	77 ASD 77 TC (ABIDE)	rsfMRI	CC200	Pearson	SVM	63%	62%	64%
Guo et al. (2017)	55 ASD 55 TC (ABIDE)	rsfMRI	AAL	Pearson	DNN	86.36%	Unknown	Unknown
Dvornek et al. (2017)	539 ASD 573 TC (ABIDE)	rsfMRI	Time series	None	LSTM	68.5%	Unknown	Unknown
Abraham et al. (2017)	403 ASD 468 TC (ABIDE)	rsfMRI	MSDL	Tangent	SVM	67.9%	58.1%	76.6%
Heinsfeld et al. (2018)	505 ASD 530 TC (ABIDE)	rsfMRI	CC200	Pearson	DNN	70%	74%	63%
Yao et al. (2019)	485 ASD 544 TC (ABIDE)	rsfMRI	BASC/ Power	Pearson	MTGCN	67.30%	64.20%	70.40%
Zhao et al. (2019)	303 ASD 390 TC (ABIDE)	rsfMRI	RSNs	None	CNN	65.30%	Unknown	Unknown
Lu et al. (2020)	505 ASD 530 TC (ABIDE)	rsfMRI	CC200	Pearson	AE-MKFC	61.00%	Unknown	Unknown
Yin et al. (2021)	403 ASD 468 TC (ABIDE)	rsfMRI	Power	Pearson	DNN	79.2%	Unknown	Unknown
Yang et al. (2021)	79 ASD 105 TC (ABIDE)	rsfMRI	group ICA	None	CNN	77.74%	78.57%	Unknown
Wang et al. (2022)	280 ASD 329 TC (ABIDE)	rsfMRI	BASC	Pearson	MC-NFE	68.42%	70.05%	63.34%
Zhang, Feng, Han, Gong, and Duan (2022)	505 ASD 550 TC (ABIDE)	rsfMRI	CC200	Pearson	DNN	70.90%	Unknown	Unknown

a classification feature to classify 871 resting-state functional magnetic resonance imaging (rs-fMRI) samples extracted from the ABIDE multisite repository. Our methodology and results have three main parts. First, we investigate 8 different brain parcellation techniques used for ASD classification, including structural, functional, and data-driven based brain parcellation techniques. Second, we evaluate three metrics of functional connectivity, including correlation, partial correlation, and tangent-space. Third, we compare and summarize four supervised learning models used in the field of ASD classification. In conclusion, we found that the functional brain network atlas BASC44 and Radial Basis Function (RBF) kernel SVM model in combination with the correlation metric are the best-integrated approach.

2. Brain network

Our brain is a complex network composed of functional and structural interconnected regions. Thus, brain networks can be divided into structural and functional networks. Different brain atlases can be applied for the same neuroimaging data to identify network properties and assist in locating various conditions or pathologies. This means that the brain atlas is a critical factor in the reliability of brain network analysis and appropriate atlases are helpful to combine the analysis of structural and functional networks (Yao, Hu, Xie, Moore, & Zheng, 2015).

2.1. Predefined atlases

In the analysis of structural and functional networks, some predefined parcellation atlases, such as Harvard-Oxford (HO) and the automated anatomical labeling (AAL) atlases, have been widely used in fMRI data analysis (Craddock, James, Holtzheimer, Hu, & Mayberg, 2012; Khazaee, Ebrahimpour, & Babajani-Feremi, 2016; Riaz et al., 2018; Rosa et al., 2015; Schouten et al., 2016). However, most of these atlases were derived from anatomical landmarks or cyto-architectonic boundaries providing little connectivity information effectively making their ability to accurately interpret connectomes limited. Since these anatomical atlas approaches have reliability and suitability issues involving connectivity, scientists have now turned their interest toward functional relationships between brain regions. Some functional atlases have been proposed, such as BASC, Power 264-region atlas, and CC200/CC400. Regions of Interest (ROIs) generated from this parcellation, such as CC200/CC400, outperform the anatomical atlas (AAL, HO) in the context of resting-state functional connectivity analysis.

In 2010, the Bootstrap Analysis of Stable Clusters (BASC) atlas was proposed in Bellec, Rosa-Neto, Lyttelton, Benali, and Evans (2010). This atlas was generated from group brain parcellations using the BASC method, which is an algorithm based on K-means clustering to identify brain networks with coherent activity in resting-state fMRI (Arco, Diaz-Gutierrez, Ramirez, & Ruz, 2020). BASC uses a variation of the Bootstrap method called circular block bootstrap (CBB) (Efron & Tibshirani, 1994) to resample time blocks to form surrogate time series, and K-means to generate the adjacent matrices. Finally, the average

Table 2

Brain atlas list.

Structural atlas	
Automated Anatomical Labeling (AAL)	116 ROIs
Functional atlas	
CC200	200 ROIs
CC400	400 ROIs
Power 264	264 ROIs
Bootstrap Analysis of Stable Clusters (BASC 197)	197 ROIs
Bootstrap Analysis of Stable Clusters (BASC 444)	444 ROIs
Data-driven method	
Canonical Independent Component Analysis (CanICA)	20 ICs
Dictionary Learning (DictLearn)	20 ICs

of the replicated adjacent matrices will be taken as the function connectivity matrix. Based on this framework, different region of interest (ROI) versions of atlases was constructed dependent upon the number of networks defined. In this study, we used two regions of interest (ROI) versions involving 444 and 197 regions.

Power and his colleagues proposed a functional template called Power 264-region atlas in 2011 where the whole-brain atlas is labeled across 264 ROIs using a graph-theoretical method. Power's 264-region atlas has been divided into 13 functional networks using resting-state fMRI (Power et al., 2011).

2.2. Data-driven method

In 2012, Craddock and his colleagues introduced a data-driven method for generating brain atlases by parcellating whole-brain resting-state fMRI data into spatially coherent regions of homogeneous functional connectivity (Craddock et al., 2012).

We studied two popular data-driven methods to extract brain ROIs from resting-state fMRI data: Canonical Independent Component Analysis (CanICA) and Dictionary Learning (DictLearn). The paper (Varoquaux, Baroni, Kleinschmidt, Fillard, & Thirion, 2010) presented a multivariate two-level generative model called CanICA to extract group-level ICA map modeling subject variability. The strength of CanICA is that it can use generalized canonical correlation analysis (CCA) to identify a subspace of reproducible components across subjects. Compared to other group models such as concatenation and tensorial group ICA, CanICA is auto calibrated and can extract meaningful, reproducible features from fMRI data by means of automation.

Typically, the initial step for resting-state fMRI data analysis is to decompose the 4D time-series data into a sum of spatially located functional networks. These functional networks represent a set of brain activation maps and were widely used for feature extraction prior to statistical learning. Initially, independent component analysis (ICA) was the most popular technique for decomposition. In 2016, Mensch and his colleagues demonstrated that improved results can be obtained using dictionary learning algorithms for fMRI data (Mensch, Varoquaux, & Thirion, 2016). They confirmed that time-reduced dictionary learning produces a result as reliable as non-reduced decompositions.

Our approach explores the efficacy of both anatomically and functionally defined reference brain atlases as well as data-driven methods to define the ROIs. To pinpoint the preferred brain atlas for ASD classification, we evaluate each atlas' cross-validation sensitivity, specificity, and accuracy. The eight evaluated atlases are listed in Table 2.

Across different experimental modalities, the functional atlas approach outperformed structural atlas and data-driven generated atlas. The functional atlas CC400 and BASC444 are the best two atlases among all candidates. For the BASC atlas, its 444 ROI versions had marked improvement over the 197 ROI version. Fig. 1 shows the BASC 444 ROIs extract from the ABIDE dataset.

3. Resting-state functional connectivity

The initial development of the fMRI technique was driven by researchers interested in the brain's response to a specific external events or mental stimulus. As a result, most initial research has focused on the measurement of responses evoked by external events. However, with the rare exception, task-related fMRI has failed to fulfill its promise in clinical application (Greicius, 2008). The traditional fMRI protocols require design studies to examine one specific component of a cognitive system at a time. In addition, the important pathological factors are most likely to be found in patients who are seriously sick. However, usually severely sick patients often cannot perform tasks correctly in the scanner environment. This constitutes a great limitation for cognitive disease such as Autism, Schizophrenia, and Alzheimer's disease. In resting-state fMRI studies, patients do not have to perform an external task. Instead, they are usually asked to rest with their eyes closed. Therefore, resting-state functional connectivity is a relatively novel method with the potential advantage to overcome these limitations in conventional fMRI protocols.

Functional connectivity is defined as the temporal correlation of a neurophysiological index measured in different brain areas in the context of functional neuroimaging (Friston, Frith, Liddle, & Frackowiak, 1993). The neurophysiological index is measured using the Blood Oxygen Level-Dependent (BOLD) signal recorded in fMRI, which shows low-frequency spontaneous fluctuations when the brain is at rest state. These low-frequency spontaneous fluctuations show a high degree of temporal correlation in distributed brain regions (Greicius, Sukekar, Menon, & Dougherty, 2009). These temporal correlations are assumed to reflect inherent functional connectivity and have been demonstrated in different brain network studies which related to vision, hearing, and language function (Beckmann, DeLuca, Devlin, & Smith, 2005; Hampson, Peterson, Skudlarski, Gatenby, & Gore, 2002; Seeley et al., 2007).

Since these landmark discoveries, an increasing number of fMRI studies are using the temporal correlation of low-frequency fluctuations between brain regions to reflect the variations in neuronal activity inferring functional connectivity. Changes in functional connectivity have been investigated in numerous psychiatric and neurological disorders, including Alzheimer's disease (Li et al., 2002; Wang et al., 2006), schizophrenia (Bluhm et al., 2007; Garrity et al., 2007; Zhou et al., 2007), depression (Hampson et al., 2005), and autism spectrum disorder (ASD) (Cherkassky, Kana, Keller, & Just, 2006; Just et al., 2004; Kennedy & Courchesne, 2008). Particularly in ASD studies, decreased connectivity in ASD have been found using data from resting state fMRI (Cherkassky et al., 2006; Kennedy & Courchesne, 2008).

To calculate functional connectivity, we estimate the sample covariance matrix of each subject's time-series signal (Pervaiz, Vidaurre, Woolrich, & Smith, 2020). Recall that we are studying three different parametrizations of functional connectivity: full correlation, partial correlation, and tangent-space. Mathematically, full correlation is a standardized form of covariance whose values exist between -1 and +1. Partial correlation is calculated from the inverse of the covariance matrix. Given covariance matrix Σ and the inverse of the covariance matrix $\Gamma = \Sigma^{-1}$, the partial correlation coefficients can be readily calculated by $\Pi_{ij} = -\frac{\Gamma_{ij}}{\sqrt{\Gamma_{ii}\Gamma_{jj}}}$, where i and j are two distinct regions, and $\Pi_{ii} = 1$. The tangent-space parameterization is the middle ground between full and partial correlation. It consists of several steps. First, a group representative covariance matrix is constructed from the mean effect on the covariance matrix of the training data. Then we whiten (or uniformly diagonalize) the data's covariance matrix through a product involving negative fractional powers of the group representative matrix and its transpose. This is followed by taking the matrix logarithm (Varoquaux, Sadaghiani, et al., 2010).

For each parameterization, we vectorize the functional connectome using the lower triangular part of the connectivity matrix for classification. Fig. 2 shows the correlation matrix of a single ASD subject using brain atlas AAL.

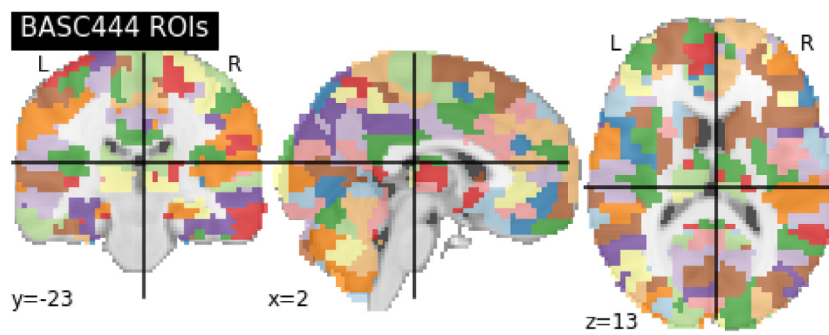


Fig. 1. BASC444 ROIs.

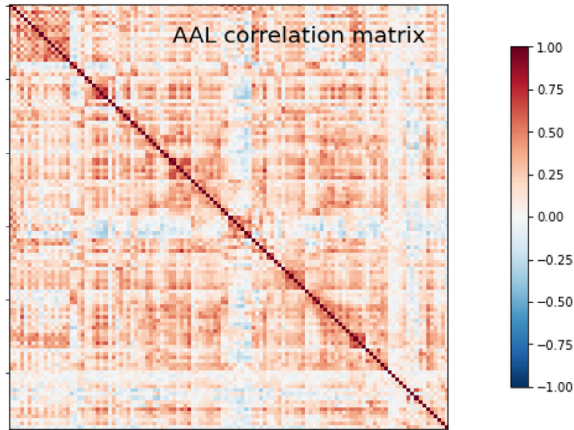


Fig. 2. AAL Correlation matrix.

4. Machine learning methods

The behavioral phenotype of ASD has been well-depicted but its etiology and pathology is still unclear (Kennedy & Courchesne, 2008). According to the study of Hallmayer et al. the causes of ASD mainly include genetic and environmental factors (Hallmayer et al., 2011). The conventional clinical methods have elucidated many aspects of ASD. However, it is still inadequate for distinguishing ASD from healthy controls (Cherkassky et al., 2006). To help traditional clinical methods augment and expand existing knowledge in ASD, machine learning was introduced in the neuroimaging field. Machine learning algorithms have been successfully applied to diagnose a wide range of neurological and psychiatric diseases such as alzheimer's disease (Cuingnet et al., 2011), schizophrenia (Arbabshirani, Kiehl, Pearson, & Calhoun, 2013; Yang, Liu, Sui, Pearson, & Calhoun, 2010) and autism spectrum disorder (Bi, Wang, Shu, Sun, & Xu, 2018; Mwangi, Ebmeier, Matthews, & Douglas Steele, 2012). These results indicate that machine learning methods have the potential to provide supplementary information for clinical practice and research and make accurate predictions. Furthermore, machine learning may identify objective biomarkers based on abnormalities of brain structure (Cherkassky et al., 2006).

In our approach, once we have extracted the connectivity features from the ROIs, the next step is to train the model using machine learning methods. Machine learning can be broadly divided into two categories, unsupervised and supervised learning. This paper focuses on the supervised learning methods. Supervised learning involves algorithms that use input variables to predict a target classification. A supervised learning algorithm analyzes the training data to learn the mapping function that can be used to classify new examples.

4.1. Supervised learning classifiers

Traditionally, fMRI analysis methods have focused on characterizing the relationship between cognitive variables and individual brain voxels. However, there are limits on what can be learned about cognitive states by examining voxels in isolation. Since 2006, when Norman and his colleagues introduced the concept of multi-voxel pattern analysis, MVPA has become a very common method for neuroimaging data analysis.

Machine learning scientists have developed a broad range of classification algorithms that can be used in MVPA studies, including linear and non-linear classifiers such as gaussian naïve bayes, linear discriminant analysis, nearest neighbor, logistic regression, linear support vector machines (SVM) and kernel SVM (Rosa et al., 2015; Schouten et al., 2016; Zou et al., 2019). Among these, SVMs have become popular as supervised classifiers for fMRI data due to its high performance. SVMs were initially motivated to deal with small sizes and high-dimensional inputs, which match the situation involved in fMRI data (LaConte, Strother, Cherkassky, Anderson, & Hu, 2005). SVMs have been applied successfully to a wide range of problems in fMRI studies (Duda et al., 2012; Kana et al., 2011).

In the studies of Autism, SVM has been successfully applied to classify ASD from healthy controls. In 2015, Jin et al. proposed an original multi-kernel SVM classification method, which can classify ASD from TD with an accuracy rate of 76%, 40 high-risk infants and 40 low-risk infants were used in this study (Jin et al., 2015). Chen et al. in 2016 used the SVM to identify ASD from TD and the accuracy rate can reach to 79.17%, which studied 112 ASD and 128 TD adolescents (Chen et al., 2016). Also, Odriozola et al. used the SVM to classify ASD from TD based on functional magnetic resonance imaging (fMRI) data with 20 ASD children and 20 typically developing (TD) peers, and the classification accuracy is 85% (Odriozola et al., 2016).

These SVM classification studies on ASD have obtained relatively high classification accuracy. However, we must point out that the sample size of these studies is small. In this paper, we address this issue by studying a relatively large sample size with 871 rs-fMRI samples downloaded from the ABIDE multisite repository.

There is a large amount of literature devoted to developing novel classifiers in fMRI and claiming its improved performance over other methods. However, even though a specific classifier may apply to a particular dataset or problem, no single method is superior in all datasets and classification problems. Therefore, it is vital to test a series of classifiers to ensure that any results are not governed by the classifier being studied. In this investigation we compared four different machine learning classifiers: logistic regression (LR), linear SVM (lSVM), kernel SVM (kSVM), and deep neural network (DNN).

4.2. Logistic regression

Logistic regression is a statistical model that uses a logistic function to model a binary dependent variable. Logistic regression is commonly

used to estimate the probability that an instance belongs to a certain category (usually the positive class, labeled “1”). In our case, what is the probability of a subject being autism? For each subject, the model outputs a probability between 0 and 1. When the probability is greater or equal to 0.5, this subject will be diagnosed as autism. The logistic regression model can be written in the following mathematical form:

$$P(x) = \frac{1}{1 + e^{-(x^T \theta)}}, \quad (1)$$

where e is the base of the natural logarithm, θ is the vector of the parameters (including weights and bias) of the model. The parameters are estimated using the training data. The output of the logistic function is used to assign the category of the new observation.

4.3. Support Vector Machine

Support Vector Machine (SVM) is a very powerful and widely used machine learning model for both classification and regression problems. The objective of an SVM classifier is to find a hyperplane in an p -dimensional space that distinctly separate the two classes, where each instance has p features. Support vector classifier is also known as maximal marginal classifier, which means the hyperplane not only separates the two classes but also stays as far away from the closest training instances (the support vectors) as possible. In our case, we will maximize the distance between the decision boundaries of the autism instances and healthy ones. SVM problem can be formulated as:

$$\min \frac{\|w\|^2}{2} \text{ such that } y_i (w \cdot x_i + b) - 1 \geq 0 \quad (2)$$

In many cases, especially for high-dimensional datasets, they are linearly separated, which means we can apply an SVM model directly to the original data and get a surprisingly good performance. For many other datasets, it becomes impossible to train a linear SVM model. One possible way to tackle nonlinearity is to add more features by using a function, such as linear function, polynomial function or Gaussian Radial Basis (RBF) function, in our experiments, we used linear SVM and SVM with RBF kernel. But it yields another problem if we add too many extra features, it makes the training process too slow. To overcome this, we can apply an amazing mathematical trick called the kernel trick to get same results as if adding extra features even without actually calculating or adding any features. A kernel function can take as its inputs vectors in the original space and returns the dot product of the vectors in the new feature space. More formally, if we add have data $x_i, x_j \in \mathcal{R}^p$ and a map $\phi: \mathcal{R}^p \rightarrow \mathcal{R}^q$, then a kernel function is defined as:

$$K(x_i, x_j) = \langle \phi(x_i), \phi(x_j) \rangle \quad (3)$$

4.4. Deep neural network

Recent research in deep learning methods shows that in the case of high-dimensional datasets such as fMRI data, deep learning models have a significant affinity for feature extraction. To date, deep learning algorithms have been successfully applied to functional connectivity-based classification studies. Xinyu Guo et al. use DNN to classify ASD and TD with 55 ASD and 55 TD adolescents, the classification accuracy is 86.36% (Guo et al., 2017). Yazhou Kong et al. apply DNN to identify ASD from TD and the accuracy rate can reach to 90.39%, which studied 78 ASD and 104 TD subjects (Kong et al., 2019). Generally, the studies with a small number of subjects from a single data site could achieve a high classification accuracy up to 90%. However, classification accuracy drops significantly when larger number of subjects from a multisite are studied. For example, only 60% classification accuracy was obtained with 964 subjects (447 ASD and 517 TD) from 16 separate international sites in Nielsen et al. (2013). 70% classification accuracy was obtained with 1035 subjects (505 ASD and 530 TD) from 17 international sites in Heinsfeld et al. (2018).

Deep learning algorithms have been widely applied to functional connectivity-based classification in neuroimaging field. However, there are still many challenges in applying deep learning to fMRI data. An important prerequisite for deep learning to provide a training sample set of sufficient size. In most fMRI data analysis, the number of training samples is limited. Recall that for this work, we have downloaded 871 rs-fMRI samples from the multisite data repository ABIDE I.

In our experimentation, we applied a DNN with eight hidden layers. The DNN accepts an input space extracted from distinct brain atlases with an output space of 2 numbers. A schematic of this DNN is seen in Fig. 3. Hidden layer 1 has 2600 nodes, hidden layer 2 has 2048 nodes, hidden layer 3 has 1024 nodes, hidden layer 4 has 512 nodes, hidden layer 5 has 256 nodes, hidden layer 6 has 128 nodes, hidden layer 7 has 64 nodes, hidden layer 8 has 32 nodes.

Observe in Fig. 3 that the DNN contains a significant number of weights. In general, the purpose of DNN is to adjust the weights for each layer through a series of epochs involving feed forward and back propagation interactions to minimize the prediction error based on a given training set. The loss function used to measure the prediction error that the model produces, and control these weight adjustments is given in Eq. (4).

$$J(\theta) = -\frac{1}{n} \left[\sum_{i=1}^n y_i \cdot \log \hat{y}_i + (1 - y_i) \log(1 - \hat{y}_i) \right] + \frac{\lambda_1}{2n} \sum_{l=1}^L \sum_{i=1}^{S_l} \sum_{j=1}^{S_{l+1}} |\theta_{ji}^{(l)}| + \frac{\lambda_2}{2n} \sum_{l=1}^L \sum_{i=1}^{S_l} \sum_{j=1}^{S_{l+1}} (\theta_{ji}^{(l)})^2 \quad (4)$$

Loss Function

ASD classification is a binary classification task. Thus, the loss function we used here is the softmax cross-entropy with logits. All cross-validation training and testing processes are implemented under the deep learning framework TensorFlow computed on a GPU containing a NVIDIA GeForce RTX 2080 Super. In addition, to optimize the cost, we employed the Adam optimizer. To address any overfitting issues, we add an l_1 and l_2 regularization term for each layer's weights in the loss function. In Eq. (1), n is the total number of the training samples ($n = 871 * 0.8 = 696$), L is the total number of DNN's layers ($L = 8$), λ_1 is the coefficient to control the l_1 penalty, λ_2 is the coefficient to control the l_2 penalty, which are determined using the grid search method. S_l is the total number of neurons in layer l ; S_{l+1} is the total number of neurons in layer $l + 1$.

5. Experiments

5.1. The ABIDE dataset

The Autism Brain Imaging Data Exchange I (ABIDE I) represent the first ABIDE initiative. ABIDE I has aggregated resting-state fMRI, structural MRI, and phenotypic datasets collected from 17 international laboratories worldwide. The ABIDE I repository consists of 1112 samples, including 539 individuals with ASD and 573 typically developing (TD) controls (Craddock et al., 2013). In accordance with the Health Insurance Portability and Accountability Act of 1996 (HIPAA) guidelines and the International Neuroimaging Data-sharing Initiative (INDI) protocols, all datasets have been completely anonymized, with no protected health information provided. More details about the dataset are available at http://fcon_1000.projects.nitrc.org/indi/abide/.

In this study, all the ABIDE I datasets are fetched using nilearn <https://nilearn.github.io/>. By disabling the quality control parameter, we can download 1035 subjects. Considering the quality issue, we downloaded 871 subjects as qualified candidates with the quality control parameter enabled. In these 871 subjects, there are 403 ASD and 468 TD subjects, of which 144 females and 727 males. The screened 871 subjects' summary information is displayed in Table 3. Table 3 illustrates the phenotypical information of lab site name, ASD/TD group, gender, total numbers, and age range in each lab site.

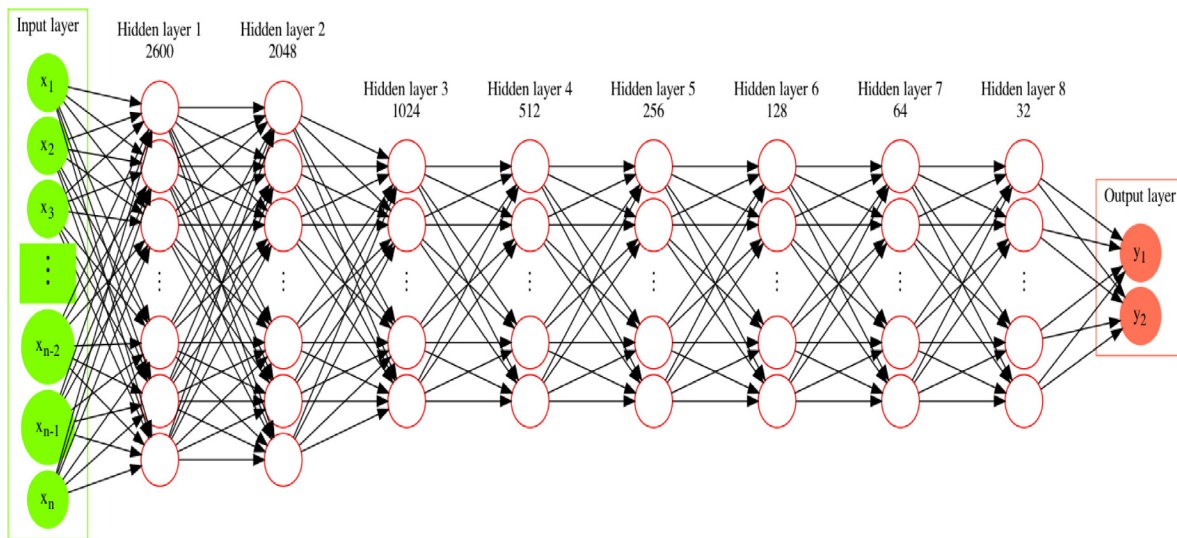


Fig. 3. DNN with eight hidden layers.

Table 3
ABIDE I data phenotypical information.

Site	Subject		Gender		Total	Age Range
	ASD	TD	M	F		
CALTECH	5	10	10	5	15	17~56
CMU	6	5	7	4	11	19~33
KKI	12	21	24	9	33	8~13
LEUVEN	26	30	49	7	56	12~32
MAX_MUN	19	27	42	4	46	7~58
NYU	74	98	136	36	172	6~39
OHSU	12	13	25	0	25	8~15
OLIN	14	14	23	5	28	10~24
PITT	24	26	43	7	50	9~35
SBL	12	14	26	0	26	20~49
SDSU	8	19	21	6	27	9~17
STANFORD	12	13	18	7	25	8~13
TRINITY	19	25	44	0	44	12~26
UCLA	48	37	74	11	85	8~18
UM	47	73	93	27	120	8~29
USM	43	24	67	0	67	9~50
YALE	22	19	25	16	41	7~18
TOTAL	403	468	727	144	871	6~58

5.2. Data preprocessing

The main purpose of preprocessing is to reduce the effects of artifacts and other noise in preparation for functional connectivity analysis. Data from ABIDE I are preprocessed using four different strategies: Configurable Pipeline for the Analysis of Connectomes (CPAC), Connectome Computation System (CCS), the Data Processing Assistant for Resting-State fMRI (DPARSF), and the NeuroImaging Analysis Kit (NIAK). According to our previous study in Yang, Schrader, and Zhang (2020), the dataset preprocessed with CPAC obtained the highest performance of those studied. Therefore, in this study, we have implemented the experiments with the dataset preprocessed using CPAC. CPAC is an open-source software pipeline for automated preprocessing and analysis of resting-state fMRI data, which includes slice time correction, motion correction, temporal filtering, skull stripping, nuisance regression, normalization, and registration. Functional images were registered to anatomical space by a linear transformation, followed by white matter boundary-based transformation using FMRIB's Linear Image Registration Tool (FLIRT) of FMRIB Software Library (FSL) and white matter tissue segmentation of FAST. More details about the CPAC, CCS, DPARSF, and NIAK preprocessing (Craddock et al., 2013) can be found at: <http://preprocessed-connectomes-project.org/abide/Pipelines.html>

5.3. Experimental design pipeline

Fig. 4 shows the experimental design pipeline we implemented in this study. In the first step, we extract ROIs time series from the preprocessed fMRI data using different brain parcellation techniques listed in Table 2. Step 2, we calculate the functional connectivity matrix of the selected ROIs using three different kind of connectivity parameters: correlation, partial correlation, and tangent-space. In the third step, for each connectivity parameter, we vectorize the functional connectivity using the upper triangular part of the connectivity matrix for classification. Then we build the classification model with the training data and evaluate its generalization performance with the test data. We tested four different classification models in this study: Logistic Regression, linear SVM, kernel SVM and DNN. In order to obtain the optimal results, we first select the optimal hyperparameters for each classifier using the grid search method. Then, we use the selected optimal parameters for training and testing.

5.4. Five-Fold-Cross-Validation (FFCV)

To accurately assess the classifier's performance when generalizing to new data, it is critical that we use separate datasets to train and test the classifier. Our experience has shown that cross-validation appears

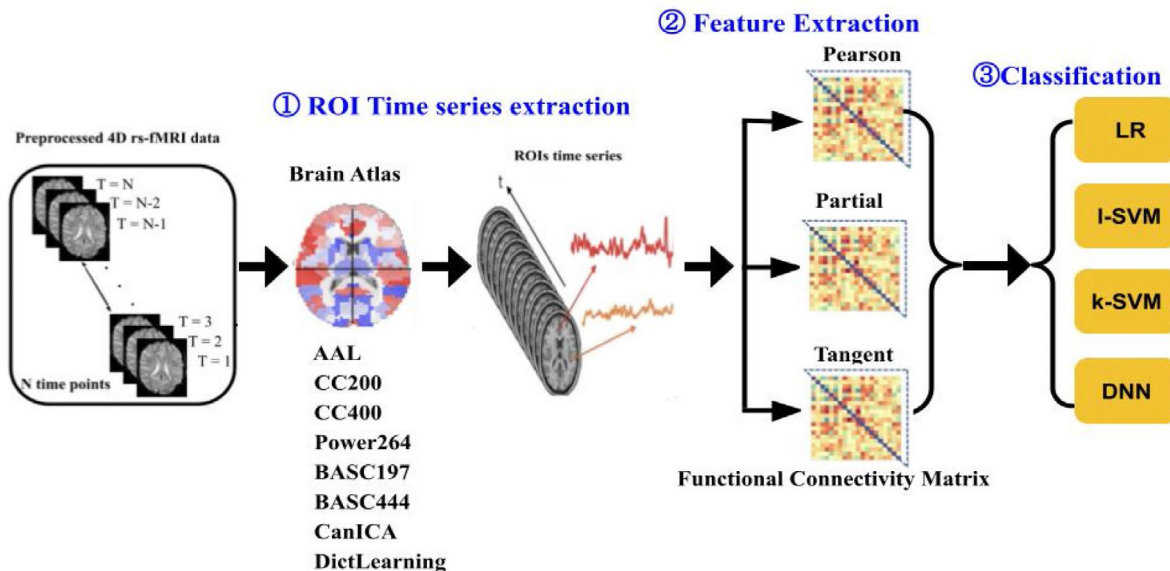


Fig. 4. Experimental Design Pipeline.

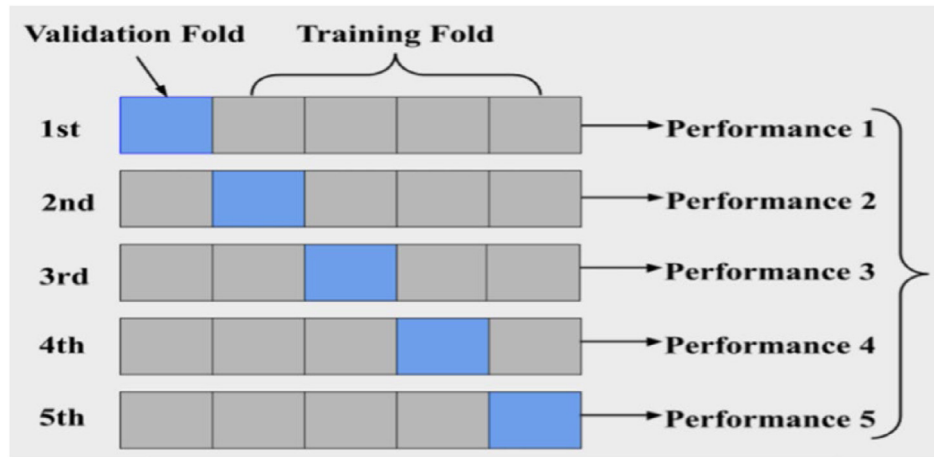


Fig. 5. Five-fold-cross-validation.

to be the optimal choice to assess the classifiers performance in generalization to new data. The K -fold cross-validation strategy divides the available data into K -subsets and trains the model on all but one of the subsets and test on the remainder.

In this study, we use five-fold-cross-validation (FFCV) to evaluate the learning performance for all classifiers. The training data are randomly partitioned into five parts. A single part is retained for validating the model and the remaining four parts are used as training data to train the model. The FFCV procedure produces five results, and these results can be averaged to obtain the final performance estimation.

$$\text{performance} = \frac{1}{5} \sum_{i=1}^5 \text{performance}_i \quad (5)$$

Fig. 5 illustrates the process of FFCV:

To obtain more stable and unbiased results, we repeated the entire five-fold cross-validation process 10 times. The final reported experimental results are the mean and standard deviation of the ten replications. We tried five-fold cross-validation with and without stratified, and the results were not much different. The results we report in this paper are results that were not stratified.

5.5. Receiver Operating Characteristic (ROC) Curve

A further measurement of a supervised machine learning model's success is area under the receiver operations character curve (ROC). A ROC curve is a graphical plot showing a binary classifier's performance. The ROC curve plots True Positive Rate (TPR) against False Positive Rate (FPR) at different classification thresholds. Recall that the TPR is also known as Sensitivity. The FPR can be calculated as (1-Specificity).

TPR is defined as follows:

$$\text{TPR} = \frac{\text{TP}}{\text{TP} + \text{FN}}$$

FPR is defined as follows:

$$\text{FPR} = \frac{\text{FP}}{\text{FP} + \text{TN}}$$

Table 4 shows the definition of True Positive (TP), True Negative (TN), False Positive (FP), False Negative (FN) via a confusion matrix:

If the patient is confirmed to have autism and the predicted result also indicates the presence of the disease, then the predicted result is a true positive (TP). Similarly, if it is confirmed that the patient does not have autism, and the predicted result also indicates that there is no disease, then the predict result is a true negative (TN). False positives and false negatives indicate that the predicted results are not consistent

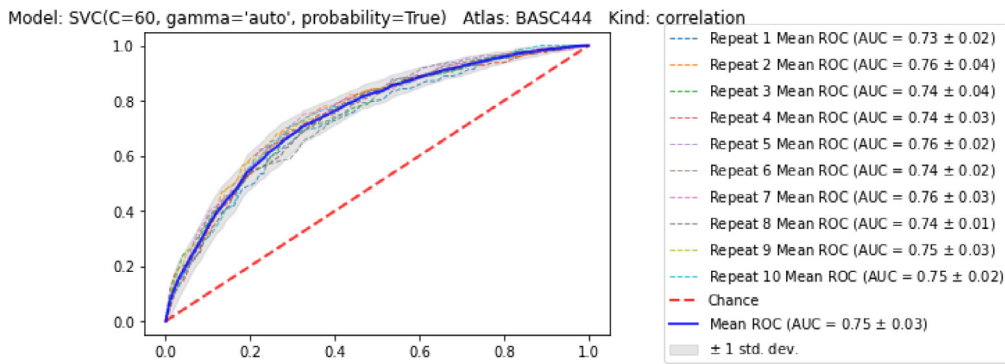


Fig. 6. Cross-validation ROC for BASC444 with correlation and RBF kernel SVM.

Table 4
Confusion matrix.

		True class	
		P	N
Predicted class	Y	TP (True Positive)	FP (False Positive)
	N	FN (False Negative)	TN (True Negative)

with the actual situation. If a person without autism is predicted to be autistic, then the prediction result is false positive (FP). Similarly, if the predicted result indicates that the patient with autism is disease-free, then the predicted result is false negative (FN).

The ROC curve is useful because it visually represents the trade-offs between the benefits (TPR) and costs (FPR) of classification. The area under the ROC curve is a measure of how well a binary classifier can distinguish between two diagnostic groups. ROC curves are also used in clinics to choose the most appropriate cut-off for testing. The best cut-off has the highest TPR along with the lowest FPR.

5.6. Experimental results

Recall that our benchmark studies explored eight different brain parcellation techniques for the ASD classification, including structural atlas, functional brain atlas and data-driven generated brain atlas. For each brain atlas, we compared four different supervised learning classification algorithms, and three different functional connectivity metrics. To obtain more stable and reliable results, we repeated the procedure of five-fold cross-validation 10 times. The five-fold-cross-validation results and standard deviation for all brain atlases can be found in Tables 5–8. The codes and results for the experiment in this paper can be found at the following GitHub link: https://github.com/XinYangMTSU/A_Study_of_ASD_Classification

From these tables, we find the highest specificity in Table 5, at 82.22%. This was achieved using a partial correlation parameterization together with the function method Power, and logistic regression. However, its corresponding sensitivity is only 43.32%. Therefore overall, this is not the best result.

The highest accuracy 69.79% is identified in Table 6 which is achieved using a tangent metric with functional atlas BASC197 and the logistic regression classifier. However, the corresponding sensitivity is not the highest.

We found that the highest sensitivity 64.57% is identified in Table 7. This result was produced using the correlation metric with functional atlas BASC444 and RBF kernel SVM. The corresponding specificity is 73.61% and the accuracy is 69.43%. Overall, this is the optimal result.

Fig. 6 show the FFCV ROC curve for BASC444 (with kernel SVM and correlation), visually presenting the trade-offs between the benefits (TPR) and costs (FPR) of classification. The area under the curve (AUC) for BASC444 with kSVM and correlation is 0.75.

In order to compare each classifier, each atlas, and each functional connectivity metric more intuitively. We present all results in Fig. 7. Figs. 7.1.1, 7.1.2, and 7.1.3 show the cross-validation accuracy, sensitivity, and specificity of the logistic regression for all eight different brain atlases using correlation, partial correlation, and tangent space, respectively. Figs. 7.2.1, 7.2.2, and 7.2.3 show the cross-validation accuracy, sensitivity, and specificity of the linear SVM for all eight different brain atlases using correlation, partial correlation, and tangent space, respectively. Figs. 7.3.1, 7.3.2, and 7.3.3 show the cross-validation accuracy, sensitivity, and specificity of the RBF kernel SVM for all eight different brain atlases using correlation, partial correlation, and tangent space, respectively. Figs. 7.4.1, 7.4.2, and 7.4.3 show the cross-validation accuracy, sensitivity, and specificity of the DNN for all eight different brain atlases using correlation, partial correlation, and tangent space, respectively.

To better analyze the performance of each classifier, each metric, and each atlas. In order to better analyze the performance of each algorithm and each metric. We performed Analysis of variance (ANOVA) tests on all results. The results of all tests are shown in Figs. 8, 9 and 10.

From Fig. 8, we can clearly see that the correlation parameterization is the best performing metric. The overall performance of the tangent space parameterization is also good, but overall, not as good as correlation parameterization. The partial correlation parameterization is the most unstable metric.

In terms of specificity, the partial correlation and tangent-space metric achieve higher performance than correlation. However, this is at the cost of sensitivity, a very important factor in ASD classification. When considering testing for ASD identification high sensitivity is preferable. Misdiagnosed cases of ASD could lead to delays in treatment, negatively affecting a patient's quality of life. Therefore, we recommend correlation metric is the best candidate among all three candidates for functional connectivity.

From Fig. 9, we found that the functional atlases achieve better performance than structural atlas and data-driven brain atlas for the ASD classification. The CC400, BASC197 and BASC444 performed comparably in both sensitivity and accuracy. However, in terms of sensitivity, accuracy and specificity, the best performance in all three items, we believe is BASC444.

From Fig. 10, we believe that logistic regression and kernel svm have comparable performance. The linear SVM classifier performance is not much different in accuracy and sensitivity, however, in terms of sensitivity, it is slightly inferior. The interesting finding is that our dnn does not have an advantage over traditional classifiers. In order to avoid the overfitting problem of dnn, we used regularization and dropout, but the results were not satisfactory. We think the main reason is that there is not enough training data, because the main requirement of deep learning is that it requires very large data.

By comparing different classifiers, we conclude that among all the experimentally compared classifiers in this paper, the kernel support vector machine (kSVM) is the optimal classifier for classifying ABIDE

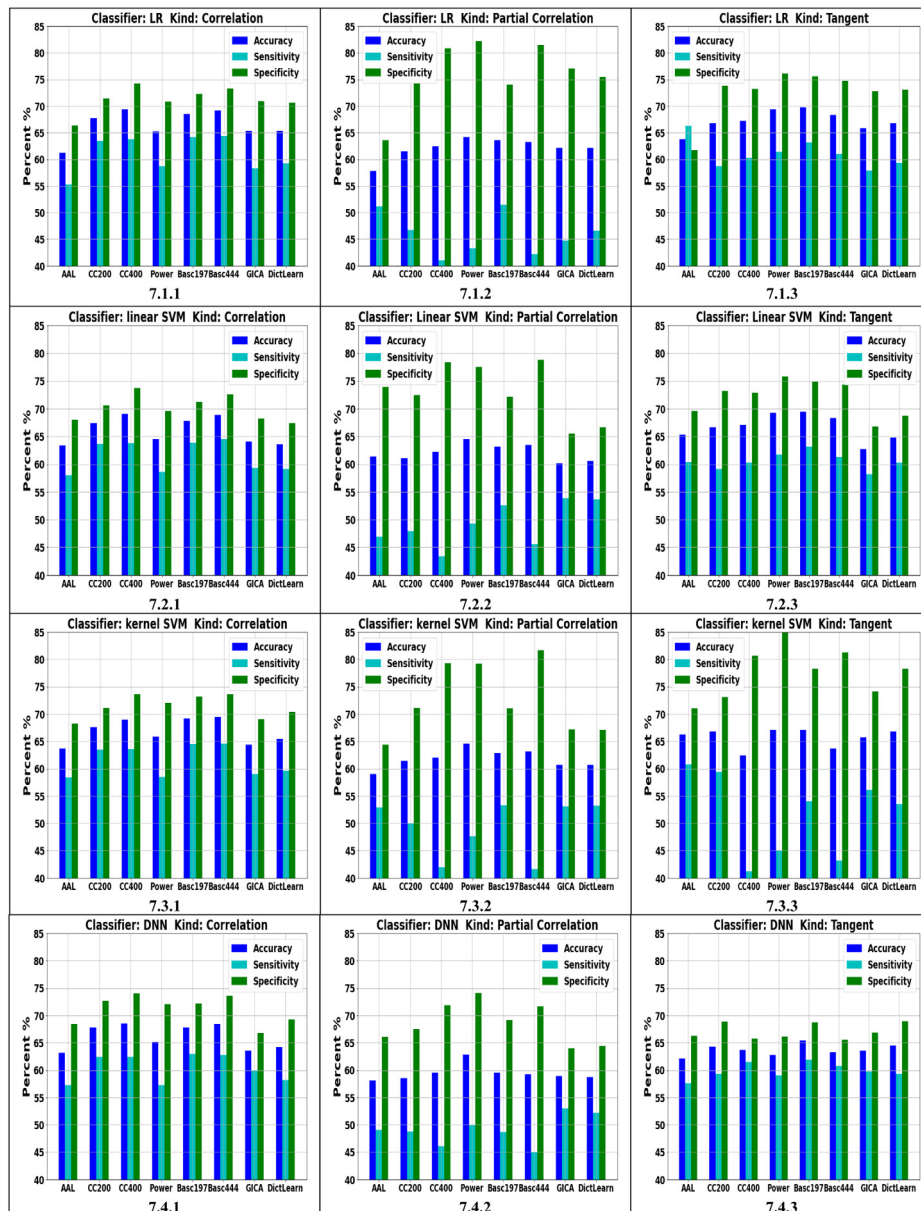


Fig. 7. Five-fold-cross-validation Results (repeat 10 times).

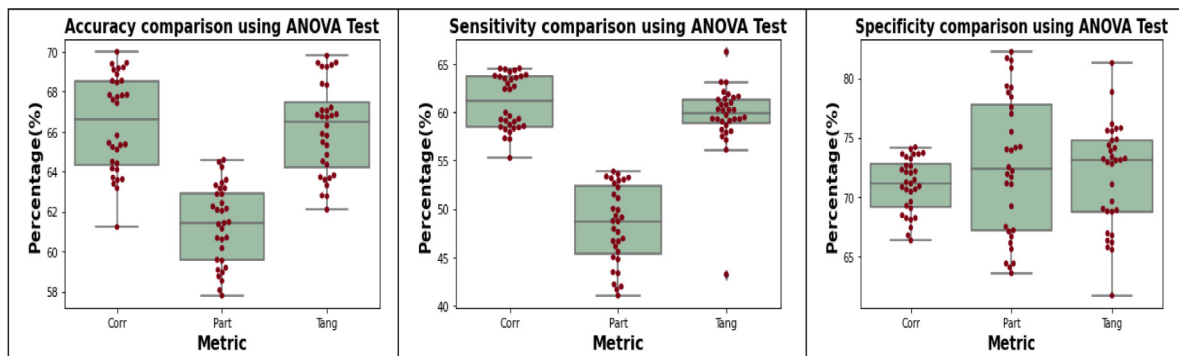


Fig. 8. Connectivity metric evaluation using ANOVA Test.

Table 5
5-fold-cross-validation results (Atlas: Power).

Atlas: Power									
Correlation				Partial correlation			Tangent		
Classifier	Sen	Spe	Acc	Sen	Spe	Acc	Sen	Spe	Acc
LR	58.73% (0.056)	70.81% (0.048)	65.22% (0.033)	43.32% (0.048)	82.22% (0.034)	64.22% (0.026)	61.41% (0.043)	76.13% (0.045)	69.32% (0.031)
ISVM	58.58% (0.058)	69.57% (0.048)	64.49% (0.036)	49.28% (0.051)	77.54% (0.041)	64.47% (0.032)	61.66% (0.041)	75.79% (0.043)	69.25% (0.029)
kSVM	58.49% (0.047)	72.09% (0.056)	65.80% (0.036)	47.59% (0.051)	79.21% (0.036)	64.58% (0.030)	58.06% (0.050)	78.84% (0.045)	69.23% (0.032)
DNN	57.31% (0.067)	72.01% (0.062)	65.09% (0.030)	49.88% (0.082)	74.14% (0.088)	62.86% (0.034)	59.05% (0.096)	66.14% (0.077)	62.76% (0.039)

Table 6
5-fold-cross-validation results (Atlas: BASC197).

Atlas: BASC197									
Correlation				Partial correlation			Tangent		
Classifier	Sen	Spe	Acc	Sen	Spe	Acc	Sen	Spe	Acc
LR	64.20% (0.052)	72.28% (0.045)	68.54% (0.030)	51.48% (0.052)	73.99% (0.044)	63.58% (0.030)	63.12% (0.047)	75.53% (0.035)	69.79% (0.026)
ISVM	63.90% (0.055)	71.21% (0.049)	67.83% (0.033)	52.65% (0.053)	72.16% (0.042)	63.14% (0.031)	63.15% (0.051)	74.83% (0.038)	69.43% (0.027)
kSVM	64.47% (0.054)	73.20% (0.045)	69.16% (0.030)	53.34% (0.052)	71.05% (0.041)	62.86% (0.032)	62.13% (0.050)	75.75% (0.038)	69.45% (0.028)
DNN	62.98% (0.054)	72.14% (0.064)	67.80% (0.033)	48.71% (0.110)	69.19% (0.107)	59.54% (0.036)	61.88% (0.0708)	68.73% (0.073)	65.47% (0.036)

Table 7
5-fold-cross-validation results (Atlas: BASC444).

Atlas: BASC444									
Correlation				Partial correlation			Tangent		
Classifier	Sen	Spe	Acc	Sen	Spe	Acc	Sen	Spe	Acc
LR	64.37% (0.054)	73.35% (0.046)	69.20% (0.029)	42.17% (0.052)	81.49% (0.040)	63.31% (0.029)	60.99% (0.048)	74.75% (0.038)	68.38% (0.028)
ISVM	64.55% (0.051)	72.58% (0.044)	68.86% (0.027)	45.55% (0.059)	78.80% (0.043)	63.42% (0.030)	61.33% (0.048)	74.34% (0.035)	68.32% (0.025)
kSVM	64.57% (0.055)	73.61% (0.045)	69.43% (0.031)	41.63% (0.047)	81.68% (0.046)	63.16% (0.027)	43.19% (0.053)	81.28% (0.045)	63.66% (0.031)
DNN	62.70% (0.067)	73.61% (0.058)	68.45% (0.031)	44.98% (0.154)	71.65% (0.131)	59.18% (0.030)	60.82% (0.097)	65.52% (0.088)	63.30% (0.039)

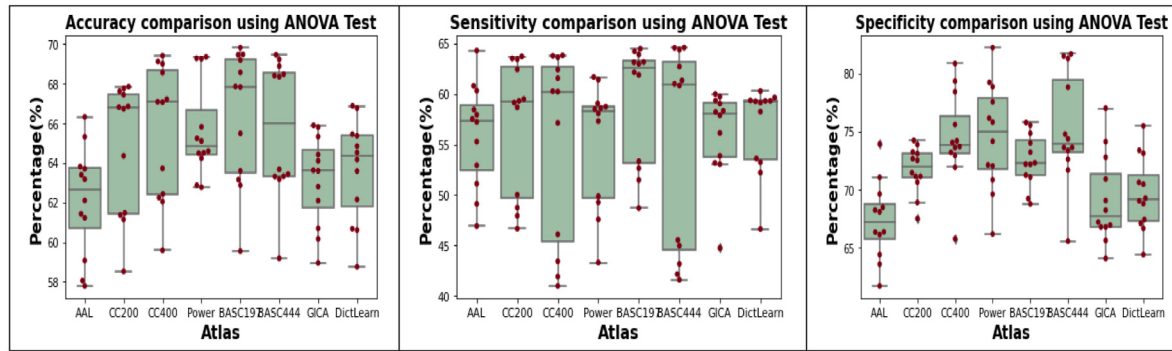


Fig. 9. Atlas evaluation using ANOVA Test.

fMRI data. The highest sensitivity 64.57% is identified in [Table 7](#). This result was produced using the correlation metric with functional atlas BASC444 and RBF kernel SVM. The corresponding specificity is 73.61%, and the accuracy is 69.43%. Overall, this is the optimal result. The optimal result is displayed in [Fig. 11\(a\), \(b\) and \(c\)](#).

Based on the above experimental results, we selected the best performing brain atlas basc444 for the analysis. We compared and analyzed the functional brain connectivity of both ASD and TD groups based on the basc444 atlas. [Fig. 12](#) illustrates the histogram of functional connectivity for both groups. Green figures show the histogram

and density of ASD group, blue figures show the histogram and density of TD group. By comparison, we found some differences in functional connectivity between the two groups, however the differences were not as pronounced as we expected.

We report five brain functional connectivity that differed most between the two groups. [Fig. 13](#) shows the location of the five most different functional connectivity in the brain. [Table 8](#) shows the coordinates of these brain functional connectivity and the corresponding brain region names. Coordinates and brain region names were matched using MRIcron software.

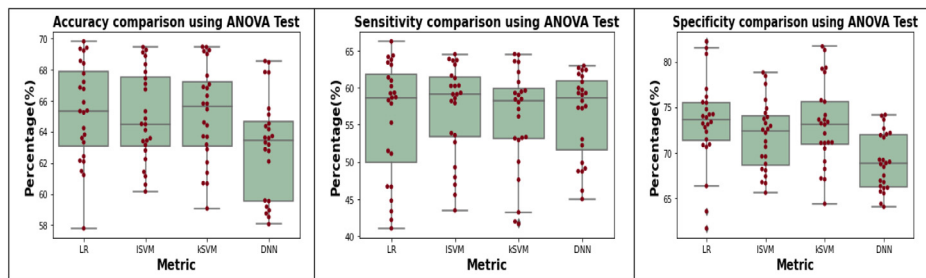


Fig. 10. Model evaluation using ANOVA Test.

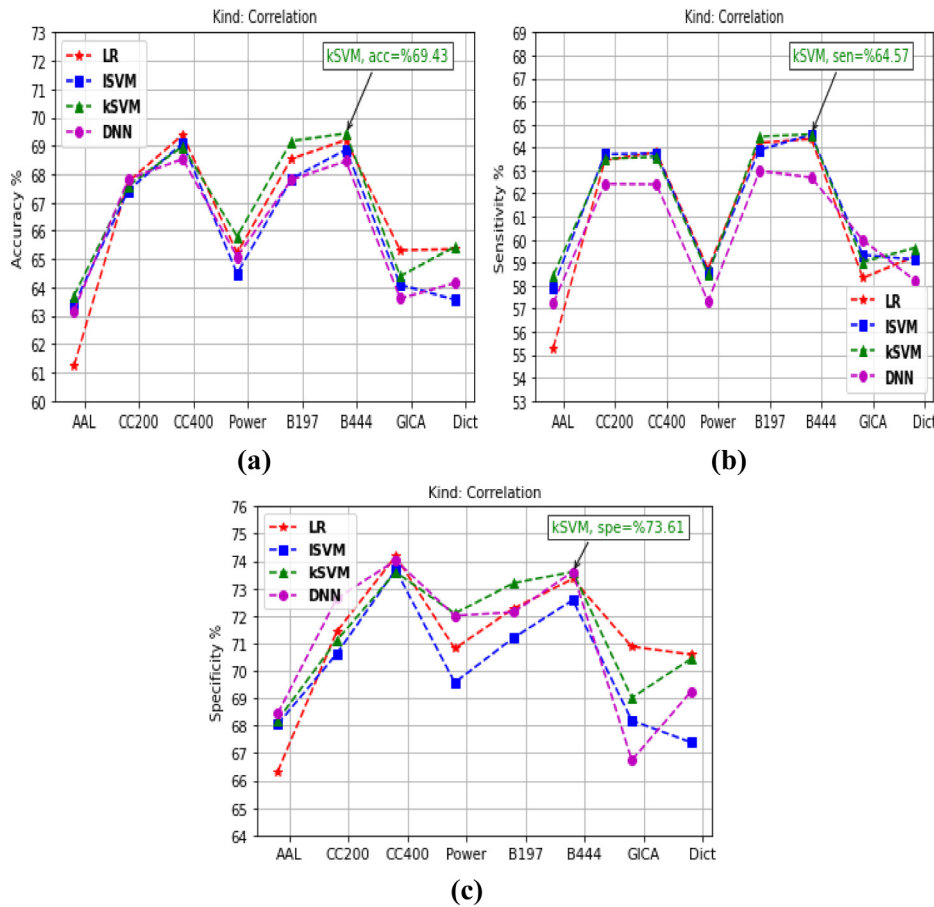


Fig. 11. Comparison of Accuracy, Sensitivity, and Specificity.

Fig. 14 shows the connectome matrix of the five most different functional connectivity. After analyzing the experimental results, we found that TD group had slightly stronger functional connectivity between the frontal cortex and cingulum than the ASD group. Cingulum is a nerve tract that allows communication between components of the frontal lobe and the parahippocampal gyrus of the temporal lobe. This is consistent with cortical under-connectivity theory; however, we did not find a very significant difference between the two groups. In addition to under-connectivity, we also found over-connectivity. We found that ASD has slightly stronger functional connectivity between temporal lobe and thalamus than the TD group. The primary function of the thalamus is to transmit motor and sensory signals to the cerebral cortex. Based on these findings, we believe that the parahippocampus and thalamus may be very important diagnostic biomarkers for autism.

6. Conclusion

This study provides a comprehensive review of existing supervised machine learning methods and brain parcellation techniques in ASD classification, which contributes to the overall understanding of ASD research. In addition to this, our findings can also be informative for clinical studies. Our results show that functional brain networks have better performance for ASD classification among all data atlases. Specifically, we identified the brain functional network BASC444 together with the correlation metric as the main candidate atlas for ASD classification. Our experimental results identified both under-connectivity and over-connectivity in ASD group, which suggests that the parahippocampus and thalamus are promising sources of biomarkers for brain pathologies in ASD. We will conduct more in-depth research on these brain areas. Furthermore, by comparing different classifiers, we found that kSVM is the best tool for fMRI classification

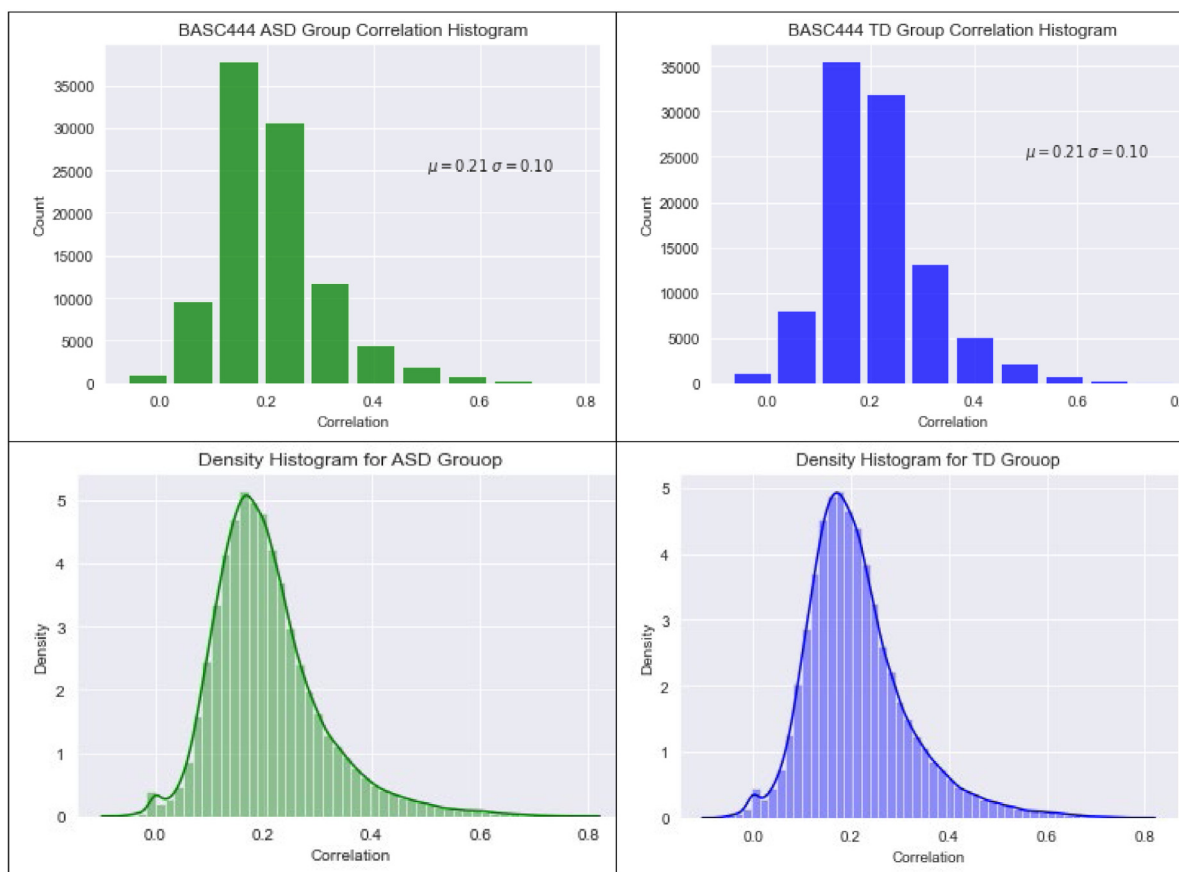


Fig. 12. Functional Connectivity Histogram for ASD and TD group.

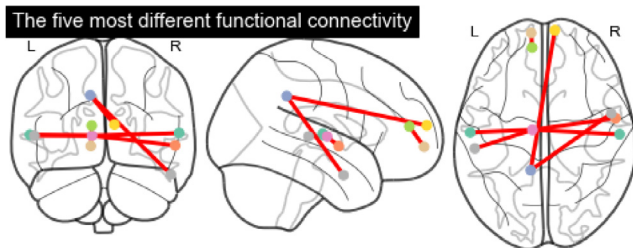


Fig. 13. The five most different functional connectivity.

in a traditional machine learning setting from an efficiency perspective. The interesting finding is that our deep neural network (DNN) model does not outperform kSVM in terms of overall performance. However, through experimental analysis, we believe that traditional machine learning has achieved the best results, and there are limitations in trying to further improve the accuracy, sensitivity, and specificity by traditional machine learning methods. From our review literature, currently the most training data is around 1000 data subjects. If we want to get a better improvement, we believe that acquiring more data and taking advantage of deep learning can lead to substantial breakthrough. The more data we have, the more complex deep learning we can construct.

With increasing computational power and the accessibility of high-performance computer (HPC) systems, deep learning will continue to exceed the threshold of classification strategies involving fMRI analysis in the future. Nevertheless, supervised deep learning requires a sufficiently large training sample set. Our further research in ASD

classification will require the collection of large amounts of training data to achieve better breakthroughs in sensitivity, accuracy, and specificity. Potential sources of this need in our ongoing experiments may include collecting additional datasets, increasing computational power, including high-performance computer (HPC) clusters, and designing more effective DNN models.

CRediT authorship contribution statement

Xin Yang: Conceptualization, Methodology, Software, Data curation, Writing – original draft, Project administration. **Ning Zhang:** Methodology, Data curation, Software, Validation. **Paul Schrader:** Visualization, Writing – review & editing.

Declaration of competing interest

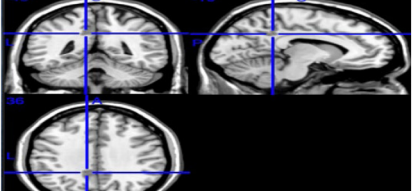
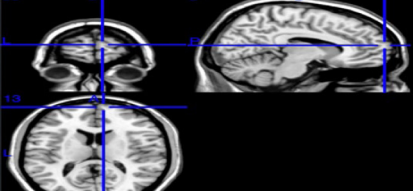
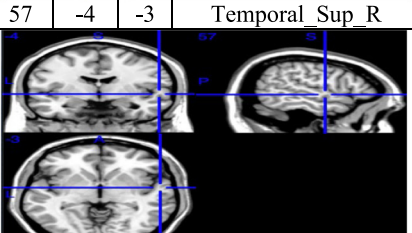
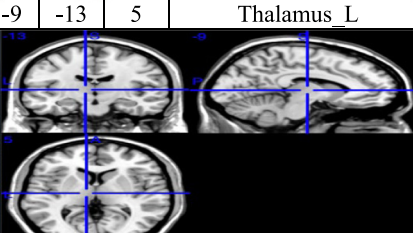
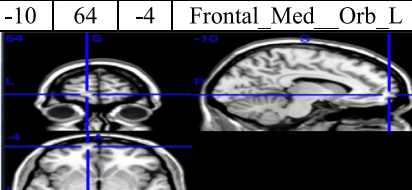
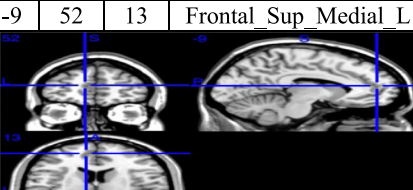
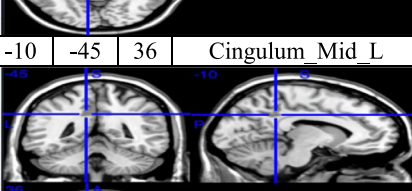
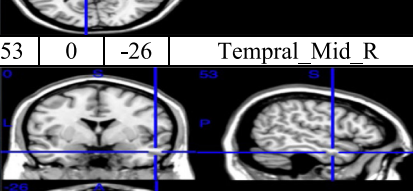
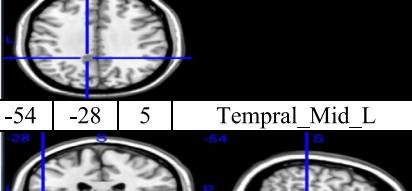
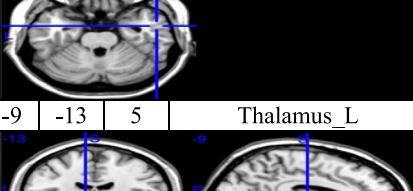
The authors declare that they have no known competing financial interests or personal relationships that could have appeared to influence the work reported in this paper.

Appendix A. Supplementary data

Supplementary material related to this article can be found online at <https://doi.org/10.1016/j.mlwa.2022.100290>.

Table 8

The five most different functional connectivity between ASD and TD using basc444.

	Region in basc444	X	Y	Z	Label Name		Region in basc444	X	Y	Z	Label Name
1	R186	-10	-45	36	Cingulum_Mid_L	↔	R244	9	66	13	Frontal_Sup_Medial_R
											
2	R169	57	-4	-3	Temporal_Sup_R	↔	R201	-9	-13	5	Thalamus_L
											
3	R257	-10	64	-4	Frontal_Med_Orb_L	↔	R204	-9	52	13	Frontal_Sup_Medial_L
											
4	R186	-10	-45	36	Cingulum_Mid_L	↔	R395	53	0	-26	Temporal_Mid_R
											
5	R441	-54	-28	5	Temporal_Mid_L	↔	R201	-9	-13	5	Thalamus_L
											

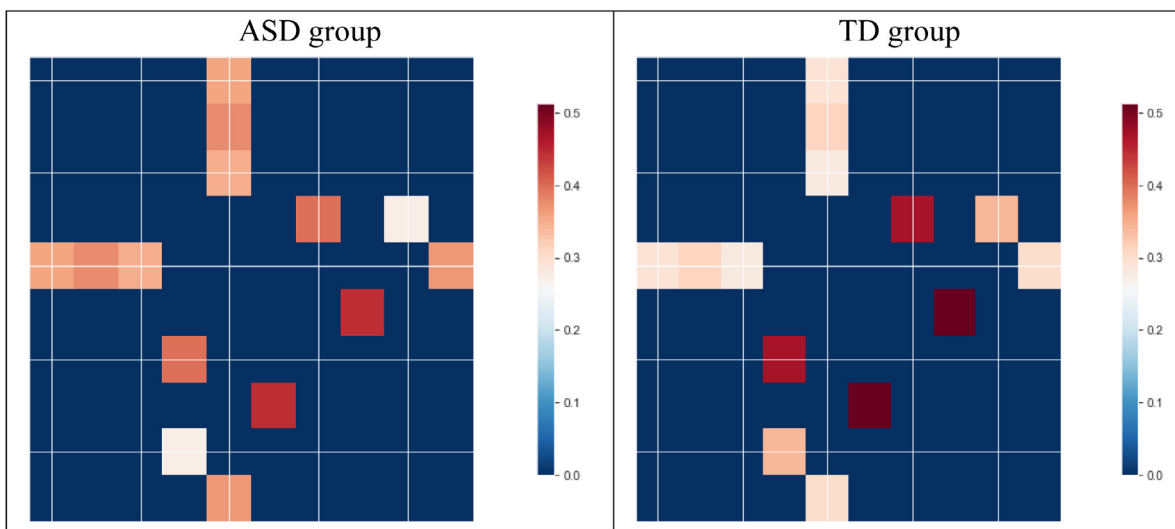


Fig. 14. Connectome matrix of the five most different functional connectivity.

References

- Abraham, A., Milham, M. P., Di Martino, A., Craddock, R. C., Samaras, D., Thirion, B., et al. (2017). Deriving reproducible biomarkers from multi-site resting-state data: An autism-based example. *NeuroImage*, 147, 736–745.
- Al-Zubaidi, A., Mertins, A., Heldmann, M., Jauch-Chara, K., & Münte, T. F. (2019). Machine learning based classification of resting-state fMRI features exemplified by metabolic state (hunger/satiety). *Frontiers in Human Neuroscience*, 13(164).
- Amodei, D., Ananthanarayanan, S., Anubhai, R., Bai, J., Battenberg, E., Case, C. . . ., et al. (2016). Deep speech 2: End-to-end speech recognition in english and mandarin. In *International conference on machine learning* (pp. 173–182). PMLR.
- Anand, A., Li, Y., Wang, Y., Wu, J., Gao, S., Bukhari, L. . . ., et al. (2005). Antidepressant effect on connectivity of the mood-regulating circuit: an FMRI study. *Neuropsychopharmacology*, 30(7), 1334–1344.
- Arbabshirani, M. R., Kiehl, K., Pearlson, G., & Calhoun, V. D. (2013). Classification of schizophrenia patients based on resting-state functional network connectivity. *Frontiers in Neuroscience*, 7(133).
- Arco, J. E., Díaz-Gutiérrez, P., Ramírez, J., & Ruz, M. (2020). Atlas-based classification algorithms for identification of informative brain regions in fMRI data. *Neuroinformatics*, 18(2), 219–236.
- Beckmann, C. F., DeLuca, M., Devlin, J. T., & Smith, S. M. (2005). Investigations into resting-state connectivity using independent component analysis. *Philosophical Transactions of the Royal Society, Series B (Biological Sciences)*, 360(1457), 1001–1013.
- Bellec, P., Rosa-Neto, P., Lyttelton, O. C., Benali, H., & Evans, A. C. (2010). Multi-level bootstrap analysis of stable clusters in resting-state fMRI. *NeuroImage*, 51(3), 1126–1139.
- Bi, X. A., Wang, Y., Shu, Q., Sun, Q., & Xu, Q. (2018). Classification of autism spectrum disorder using random support vector machine cluster. *Frontiers in Genetics*, 9(18).
- Biswal, B. B., Kylen, J. V., & Hyde, J. S. (1997). Simultaneous assessment of flow and BOLD signals in resting-state functional connectivity maps. *NMR in Biomedicine: An International Journal Devoted To the Development and Application of Magnetic Resonance in Vivo*, 10(4–5), 165–170.
- Biswal, B., Yetkin, F., Zerrin, Haughton, V. M., & Hyde, J. S. (1995). Functional connectivity in the motor cortex of resting human brain using echo-planar MRI. *Magnetic Resonance in Medicine*, 34(4), 537–541.
- Bluhm, R. L., Miller, J., Lanius, R. A., Osuch, E. A., Boksman, K., Neufeld, R. W. J. . . ., et al. (2007). Spontaneous low-frequency fluctuations in the BOLD signal in schizophrenic patients: anomalies in the default network. *Schizophrenia Bulletin*, 33(4), 1004–1012.
- Boat, T. F., & Wu, J. (2015). Committee to evaluate the supplemental security income disability program for children with mental disorders.
- Chen, H., Duan, X., Liu, F., Lu, F., Ma, X., Zhang, Y. . . ., et al. (2016). Multivariate classification of autism spectrum disorder using frequency-specific resting-state functional connectivity—a multi-center study. *Progress in Neuro-Psychopharmacology and Biological Psychiatry*, 64, 1–9.
- Chen, C. P., Keown, C. L., Jahedi, A., Nair, A., Pflieger, M. E., Bailey, B. A., et al. (2015). Diagnostic classification of intrinsic functional connectivity highlights somatosensory, default mode, and visual regions in autism. *NeuroImage: Clinical*, 8, 238–245.
- Cherkassky, V. L., Kana, R. K., Keller, T. A., & Just, M. A. (2006). Functional connectivity in a baseline resting-state network in autism. *NeuroReport*, 17(16), 1687–1690.
- Courchesne, E., Pierce, K., Schumann, C. M., Redcay, E., Buckwalter, J. A., Kennedy, D. P., et al. (2007). Mapping early brain development in autism. *Neuron*, 56(2), 399–413.
- Cox, D. D., & Savoy, R. L. (2003). Functional magnetic resonance imaging (fMRI) brain reading: detecting and classifying distributed patterns of fMRI activity in human visual cortex. *NeuroImage*, 19(2), 261–270.
- Craddock, C., Benhajali, Y., Chu, C., Chouinard, F., Evans, A., Jakab, A. . . ., et al. (2013). The neuro bureau preprocessing initiative: open sharing of preprocessed neuroimaging data and derivatives. *Frontiers in Neuroinformatics*, 7.
- Craddock, R. C., James, G. A., Holtzheimer, . P. E., III, Hu, X. P., & Mayberg, H. S. (2012). A whole brain fMRI atlas generated via spatially constrained spectral clustering. *Human Brain Mapping*, 33(8), 1914–1928.
- Cuingnet, R., Gerardin, E., Tessieras, J., Auzias, G., Lehéricy, S., Habert, M. O. . . ., et al. (2011). Automatic classification of patients with Alzheimer's disease from structural MRI: a comparison of ten methods using the ADNI database. *NeuroImage*, 56(2), 766–781.
- Damoiseaux, J. S., Rombouts, S. A. R. B., Barkhof, F., Scheltens, P., Stam, C. J., Smith, S. M., et al. (2006). Consistent resting-state networks across healthy subjects. *Proceedings of the National Academy of Sciences*, 103(37), 13848–13853.
- Doderlo, L., Sambataro, F., Murino, V., & Sona, D. (2015). Kernel-based analysis of functional brain connectivity on grassmann manifold. In *International conference on medical image computing and computer-assisted intervention* (pp. 604–611). Cham: Springer.
- Du, X., Cai, Y., Wang, S., & Zhang, L. (2016). Overview of deep learning. In *2016 31st youth academic annual conference of chinese association of automation* (pp. 159–164). IEEE..
- Duda, R. O., Hart, P. E., & D.G., Stork (2012). *Pattern classification*. John Wiley & Sons.
- Dvornek, N. C., Ventola, P., Pelphrey, K. A., & Duncan, J. S. (2017). Identifying autism from resting-state fMRI using long short-term memory networks. In *International workshop on machine learning in medical imaging* (pp. 362–370). Cham: Springer.
- Efron, B., & Tibshirani, R. J. (1994). *An introduction to the bootstrap*. CRC Press.
- Eitel, A., Springenberg, J. T., Spinello, L., Riedmiller, M., & Burgard, W. (2015). Multimodal deep learning for robust RGB-d object recognition. In *2015 IEEE/RSJ international conference on intelligent robots and systems* (pp. 681–687). IEEE.
- Eraslan, G., Avsec, Ž., Gagneur, J., & Theis, F. J. (2019). Deep learning: new computational modelling techniques for genomics. *Nature Reviews Genetics*, 20(7), 389–403.
- Formisano, E., De Martino, F., & Valente, G. (2008). Multivariate analysis of fMRI time series: classification and regression of brain responses using machine learning. *Magnetic Resonance Imaging*, 26(7), 921–934.
- Friston, K. J., Frith, C. D., Liddle, P. F., & Frackowiak, R. S. J. (1993). Functional connectivity: the principal-component analysis of large (PET) data sets. *Journal of Cerebral Blood Flow & Metabolism*, 13(1), 5–14.
- Garrity, A. G., Pearlson, G. D., McKiernan, K., Lloyd, D., Kiehl, K. A., & Calhoun, V. D. (2007). Aberrant default mode functional connectivity in schizophrenia. *American Journal of Psychiatry*, 164(3), 450–457.
- Gawehn, E., Hiss, J. A., & Schneider, G. (2016). Deep learning in drug discovery. *Molecular Informatics*, 35(1), 3–14.
- Graves, A., Mohamed, A. R., & Hinton, G. (2013). Speech recognition with deep recurrent neural networks. In *2013 IEEE international conference on acoustics, speech and signal processing* (pp. 6645–6649).
- Greicius, M. (2008). Resting-state functional connectivity in neuropsychiatric disorders. *Current Opinion in Neurology*, 21(4), 424–430.

- Greicius, M. D., Srivastava, G., Reiss, A. L., & Menon, V. (2004). Default-mode network activity distinguishes alzheimer's disease from healthy aging: evidence from functional MRI. *Proceedings of the National Academy of Sciences*, 101(13), 4637–4642.
- Greicius, M. D., Sukekar, K., Menon, V., & Dougherty, R. F. (2009). Resting-state functional connectivity reflects structural connectivity in the default mode network. *Cerebral Cortex*, 19(1), 72–78.
- Guo, X., Dominick, K. C., Minai, A. A., Li, H., Erickson, C. A., & Lu, L. J. (2017). Diagnosing autism spectrum disorder from brain resting-state functional connectivity patterns using a deep neural network with a novel feature selection method. *Frontiers in Neuroscience*, 11(460).
- Hallmayer, J., Cleveland, S., Torres, A., Phillips, J., Cohen, B., Torigoe, T., et al. (2011). Genetic heritability and shared environmental factors among twin pairs with autism. *Archives of General Psychiatry*, 68(11), 1095–1102.
- Hampson, M., Peterson, B. S., Skudlarski, P., Gatenby, J. C., & Gore, J. C. (2002). Detection of functional connectivity using temporal correlations in MR images. *Human Brain Mapping*, 15(4), 247–262.
- Hannun, A., Case, C., Casper, J., Catanzaro, B., Diamos, G., Elsen, E., et al. (2014). Deep speech: Scaling up end-to-end speech recognition. arXiv preprint arXiv:1412.5567.
- Heinsfeld, A. S., Franco, A. R., Craddock, R. C., Buchweitz, A., & Meneguzzi, F. (2018). Identification of autism spectrum disorder using deep learning and the ABIDE dataset. *NeuroImage: Clinical*, 17, 16–23.
- Hinton, G. E., & Salakhutdinov, R. R. (2006). Reducing the dimensionality of data with neural networks. *Science*, 313(5786), 504–507.
- Jang, H., Plis, S. M., Calhoun, V. D., & Lee, J. H. (2017). Task-specific feature extraction and classification of fMRI volumes using a deep neural network initialized with a deep belief network: Evaluation using sensorimotor tasks. *NeuroImage*, 145, 314–328.
- Jin, Y., Wee, C. Y., Shi, F., Thung, K. H., Ni, D., Yap, P. T., et al. (2015). Identification of infants at high-risk for autism spectrum disorder using multiparameter multiscale white matter connectivity networks. *Human Brain Mapping*, 36(12), 4880–4896.
- Just, M. A., Cherkassky, V. L., Keller, T. A., & Minshew, N. J. (2004). Cortical activation and synchronization during sentence comprehension in high-functioning autism: evidence of underconnectivity. *Brain*, 127(8), 1811–1821.
- Kana, R. K., Libero, L. E., & Moore, M. S. (2011). Disrupted cortical connectivity theory as an explanatory model for autism spectrum disorders. *Physics of Life Reviews*, 8(4), 410–437.
- Kassraian-Fard, P., Matthis, C., Balsters, J. H., Maathuis, M. H., & Wenderoth, N. (2016). Promises, pitfalls, and basic guidelines for applying machine learning classifiers to psychiatric imaging data, with autism as an example. *Frontiers in Psychiatry*, 7, 177.
- Kennedy, D. P., & Courchesne, E. (2008). The intrinsic functional organization of the brain is altered in autism. *NeuroImage*, 39(4), 1877–1885.
- Khazaee, A., Ebrahizadeh, A., & Babajani-Feremi, A. (2016). Application of advanced machine learning methods on resting-state fMRI network for identification of mild cognitive impairment and Alzheimer's disease. *Brain Imaging and Behavior*, 10(3), 799–817.
- Kim, J., Calhoun, V. D., Shim, E., & Lee, J. H. (2016). Deep neural network with weight sparsity control and pre-training extracts hierarchical features and enhances classification performance: Evidence from whole-brain resting-state functional connectivity patterns of Schizophrenia. *NeuroImage*, 124, 127–146.
- Kleinhanz, N. M., Richards, T., Sterling, L., Stegbauer, K. C., Mahurin, R., Johnson, L. C., et al. (2008). Abnormal functional connectivity in autism spectrum disorders during face processing. *Brain*, 131(4), 1000–1012.
- Kong, Y., Gao, J., Xu, Y., Pan, Y., Wang, J., & Liu, J. (2019). Classification of autism spectrum disorder by combining brain connectivity and deep neural network classifier. *Neurocomputing*, 324, 63–68.
- LaConte, S., Strother, S., Cherkassky, V., Anderson, J., & Hu, X. (2005). Support vector machines for temporal classification of block design fMRI data. *NeuroImage*, 26(2), 317–329.
- Li, S. J., Li, Z., Wu, G., Zhang, M. J., Franczak, M., & Antuono, P. G. (2002). Alzheimer disease: evaluation of a functional MR imaging index as a marker. *Radiology*, 225(1), 253–259.
- Liang, M., & Hu, X. (2015). Recurrent convolutional neural network for object recognition. In *Proceedings of the IEEE conference on computer vision and pattern recognition*, vol. 336 (pp. 7–3375).
- Lu, H., Liu, S., Wei, H., & Tu, J. (2020). Multi-kernel fuzzy clustering based on autoencoder for fmri functional network. *Expert Systems with Applications*, 159, Article 113513.
- Mensch, A., Varoquaux, G., & Thirion, B. (2016). Compressed online dictionary learning for fast resting-state fMRI decomposition. In *2016 IEEE 13th international symposium on biomedical imaging* (pp. 1282–1285). IEEE.
- Meszlényi, R. J., Buza, K., & Vidnyánszky, Z. (2017). Resting state fMRI functional connectivity-based classification using a convolutional neural network architecture. *Frontiers in Neuroinformatics*, 11(61).
- Mwangi, B., Ebmeier, K. P., Matthews, K., & Douglas Steele, J. (2012). Multi-centre diagnostic classification of individual structural neuroimaging scans from patients with major depressive disorder. *Brain*, 135(5), 1508–1521.
- Nielsen, J. A., Zielinski, B. A., Fletcher, P. T., Alexander, A. L., Lange, N., Bigler, E. D., et al. (2013). Multisite functional connectivity MRI classification of autism: ABIDE results. *Frontiers in Human Neuroscience*, 7(599).
- Norman, K. A., Polyn, S. M., Detre, G. J., & Haxby, J. V. (2006). Beyond mind-reading: multi-voxel pattern analysis of fMRI data. *Trends in Cognitive Sciences*, 10(9), 424–430.
- Odriozola, P., Uddin, L. Q., Lynch, C. J., Kochalka, J., Chen, T., & Menon, V. (2016). Insula response and connectivity during social and non-social attention in children with autism. *Social Cognitive and Affective Neuroscience*, 11(3), 433–444.
- Pervaiz, U., Vidaurre, D., Woolrich, M. W., & Smith, S. M. (2020). Optimising network modelling methods for fMRI. *NeuroImage*, 211, Article 116604.
- Poldrack, R. A., Mumford, J. A., & Nichols, T. E. (2011). *Handbook of functional MRI data analysis*. Cambridge University Press.
- Power, J. D., Cohen, A. L., Nelson, S. M., Wig, G. S., Barnes, K. A., Church, J. A., et al. (2011). Functional network organization of the human brain. *Neuron*, 72(4), 665–678.
- Riaz, A., Asad, M., Al Arif, S. M. R., Alonso, E., Dima, D., Corr, P., et al. (2018). Deep fMRI: An end-to-end deep network for classification of fMRI data. In *2018 IEEE 15th international symposium on biomedical imaging* (pp. 1419–1422). IEEE.
- Riaz, A., Asad, M., Alonso, E., & Slabaugh, G. (2020). DeepfMRI: End-to-end deep learning for functional connectivity and classification of ADHD using fMRI. *Journal of Neuroscience Methods*, 335, Article 108506.
- Rosa, M. J., Portugal, L., Hahn, T., Fallgatter, A. J., Garrido, M. I., Shawe-Taylor, J., et al. (2015). Sparse network-based models for patient classification using fMRI. *NeuroImage*, 105, 493–506.
- Schouten, T. M., Koini, M., De Vos, F., Seiler, S., Van Der Grond, J., Lechner, A., et al. (2016). Combining anatomical, diffusion, and resting state functional magnetic resonance imaging for individual classification of mild and moderate Alzheimer's disease. *NeuroImage: Clinical*, 11, 46–51.
- Seeley, W. W., Menon, V., Schatzberg, A. F., Keller, J., Glover, G. H., Kenna, H., et al. (2007). Dissociable intrinsic connectivity networks for salience processing and executive control. *Journal of Neuroscience*, 27(9), 2349–2356.
- Socher, R., Huval, B., Bath, B., Manning, C. D., & Ng, A. (2012). Convolutional-recursive deep learning for 3d object classification. *Advances in Neural Information Processing Systems*, 25, 656–664.
- Uddin, L. Q., Sukekar, K., Lynch, C. J., Khouzam, A., Phillips, J., Feinstein, C., et al. (2013). Salience network-based classification and prediction of symptom severity in children with autism. *JAMA Psychiatry*, 70(8), 869–879.
- Varoquaux, G., Baronnet, F., Kleinschmidt, A., Fillard, P., & Thirion, B. (2010). Detection of brain functional-connectivity difference in post-stroke patients using group-level covariance modeling. In *International conference on medical image computing and computer-assisted intervention* (pp. 200–208). Berlin, Heidelberg: Springer.
- Varoquaux, G., Sadaghiani, S., Pinel, P., Kleinschmidt, A., Poline, J. B., & Thirion, B. (2010). A group model for stable multi-subject ICA on fMRI datasets. *NeuroImage*, 51(1), 288–299.
- Wang, H., Chen, C., & Fushing, H. (2012). Extracting multiscale pattern information of fMRI based functional brain connectivity with application on classification of autism spectrum disorders.
- Wang, N., Yao, D., Ma, L., & Liu, M. (2022). Multi-site clustering and nested feature extraction for identifying autism spectrum disorder with resting-state fMRI. *Medical Image Analysis*, 75, Article 102279.
- Wang, L., Zang, Y., He, Y., Liang, M., Zhang, X., Tian, L., et al. (2006). Changes in hippocampal connectivity in the early stages of alzheimer's disease: evidence from resting state fMRI. *NeuroImage*, 31(2), 496–504.
- Weng, S. J., Wiggins, J. L., Peltier, S. J., Carrasco, M., Risi, S., Lord, C., et al. (2010). Alterations of resting state functional connectivity in the default network in adolescents with autism spectrum disorders. *Brain Research*, 1313, 202–214.
- Yang, M., Cao, M., Chen, Y., Chen, Y., Fan, G., Li, C., et al. (2021). Large-scale brain functional network integration for discrimination of autism using a 3-D deep learning model. *Frontiers in Human Neuroscience*, 15(277).
- Yang, H., Liu, J., Sui, J., Pearson, G., & Calhoun, V. D. (2010). A hybrid machine learning method for fusing fMRI and genetic data: combining both improves classification of schizophrenia. *Frontiers in Human Neuroscience*, 4(192).
- Yang, X., Schrader, P. T., & Zhang, N. (2020). A deep neural network study of the ABIDE repository on autism spectrum classification. *International Journal of Advanced Computer Science and Applications*, 11, 1–6.
- Yao, Z., Hu, B., Xie, Y., Moore, P., & Zheng, J. (2015). A review of structural and functional brain networks: small world and atlas. *Brain Informatics*, 2(1), 45–52.
- Yao, D., Liu, M., Wang, M., Lian, C., Wei, J., Sun, L., et al. (2019). Triplet graph convolutional network for multi-scale analysis of functional connectivity using functional MRI. In *International workshop on graph learning in medical imaging* (pp. 70–78). Cham: Springer.
- Yin, W., Mostafa, S., & Wu, F. X. (2021). Diagnosis of autism spectrum disorder based on functional brain networks with deep learning. *Journal of Computational Biology*, 28(2), 146–165.
- Zhang, J., Feng, F., Han, T., Gong, X., & Duan, F. (2022). Detection of autism spectrum disorder using fMRI functional connectivity with feature selection and deep learning. *Cognitive Computation*, 1–12.
- Zhang, L., Tan, J., Han, D., & Zhu, H. (2017). From machine learning to deep learning: progress in machine intelligence for rational drug discovery. *Drug Discovery Today*, 22(11), 1680–1685.

- Zhao, Y., Dai, H., Zhang, W., Ge, F., & Liu, T. (2019). Two-stage spatial temporal deep learning framework for functional brain network modeling. In *2019 IEEE 16th international symposium on biomedical imaging* (pp. 1576–1580). IEEE.
- Zhou, Y., Liang, M., Tian, L., Wang, K., Hao, Y., Liu, H., et al. (2007). Functional disintegration in paranoid schizophrenia using resting-state fMRI. *Schizophrenia Research*, 97(1–3), 194–205.
- Zhou, Y., Yu, F., & Duong, T. (2014). Multiparametric MRI characterization and prediction in autism spectrum disorder using graph theory and machine learning. *PLoS One*, 9(6), Article e90405.
- Zou, J., Huss, M., Abid, A., Mohammadi, P., Torkamani, A., & Telenti, A. (2019). A primer on deep learning in genomics. *Nature Genetics*, 51(1), 12–18.